Proprioceptor Regulation of Motor Circuit Activity by Presynaptic Inhibition of a Modulatory Projection Neuron

Mark P. Beenhakker
Department of Neuroscience
University of Pennsylvania School of Medicine

Nicholas D. DeLong
Department of Neuroscience
University of Pennsylvania School of Medicine

Shari Hertzberg
Department of Neuroscience
University of Pennsylvania School of Medicine

Farzan Nadim
Department of Mathematical Sciences
New Jersey Institute of Technology &
Department of Biological Sciences
Rutgers University
973-353-1541, farzan@njit.edu

Michael P. Nusbaum
Department of Neuroscience
University of Pennsylvania School of Medicine
215-898-1585, nusbaum@mail.med.upenn.edu

CAMS Report 0506-1, [Fall 2005/Spring 2006]
Center for Applied Mathematics and Statistics

Senior Editor: Barry Connors

Reviewing Editor: Ron Calabrese

August 3, 2005

Proprioceptor Regulation of Motor Circuit Activity by Presynaptic Inhibition of a Modulatory Projection Neuron

Mark P. Beenhakker[1a*]

Nicholas D. DeLong[1*]

Shari R. Saideman[1]

Farzan Nadim[2]

Michael P. Nusbaum[1]

[1]Department of Neuroscience, University of Pennsylvania School of Medicine, 215 Stemmler Hall, Philadelphia, PA 19104; [2]Department of Biological Sciences, Rutgers University & Department of Mathematical Sciences, New Jersey Institute of Technology, Newark, NJ 07102

[a]Present Address: Department of Neurology & Neurological Sciences, Stanford University School of Medicine, Stanford, CA 94305

*These Authors contributed equally to this paper.

Abbreviated Title: Proprioceptor regulation of motor circuit activity

PAGES: 49

FIGURES: 12

TABLES: 2

ABSTRACT: 250/250

INTRODUCTION: 495/500

DISCUSSION: 1519/1500

Please address all correspondence to:

Dr. Michael P. Nusbaum

Department of Neuroscience

215 Stemmler Hall

University of Pennsylvania School of Medicine

Philadelphia, PA 19104-6074

Telephone: 215-898-1585

FAX: 215-573-9050

Email: nusbaum@mail.med.upenn.edu

Acknowledgments: We thank Dawn M. Blitz for providing feedback on an earlier version of this paper. This work was supported by National Institute of Neurological Disorders and Stroke Grants NS42813 & NS29436 (MPN) and F31-NS41894 (MPB), plus grants from the National Institute of General Medical Sciences (T32-GM07517: MPN) and the National Institute of Mental Health (MH60605: FN).

Phasically active sensory systems commonly influence rhythmic motor activity via synaptic actions on the relevant circuit and/or motor neurons. Using the crab stomatogastric nervous system (STNS), we have identified a distinct synaptic action by which an identified proprioceptor, the gastro/pyloric muscle stretch receptor (GPR) neuron, regulates the gastric mill (chewing) motor rhythm. Previous work showed that rhythmically stimulating GPR in a gastric mill-like pattern, in the isolated STNS, elicits the gastric mill rhythm via its activation of two identified projection neurons, MCN1 and CPN2, in the commissural ganglia. Here, we determine how activation of GPR with a behaviorally appropriate pattern (active during each gastric mill retractor phase) influences an ongoing gastric mill rhythm via actions in the stomatogastric ganglion, where the gastric mill circuit is located. Stimulating GPR during each retractor phase selectively prolongs that phase and thereby slows the ongoing rhythm. This selective action on the retractor phase results from two distinct GPR actions. First, GPR presynaptically inhibits the axon terminals of MCN1, reducing MCN1 excitation of all gastric mill neurons. Second, GPR directly excites the retractor phase neurons. Because MCN1 transmitter release occurs during each retractor phase, these parallel GPR actions selectively reduce the buildup of excitatory drive to the protractor phase neurons, delaying each protractor burst. Thus, rhythmic proprioceptor feedback to a motor circuit can result from a global reduction in excitatory drive to that circuit, via presynaptic inhibition, coupled with a phase-specific excitatory input that prolongs the excited phase by delaying onset of the subsequent phase.

Keywords: Central Pattern Generator; Network; Gastric Mill Circuit; Stomatogastric; Neuromodulation; Sensorimotor.

Sensory influences on the central pattern generator (CPG) circuits that underlie rhythmic motor behaviors extend from phasic actions that fine-tune motor output, to the activation or termination of entire motor programs (Stein et al., 1997; McCrea, 1998; DiPrisco et al., 2000; Perrins et al., 2002; Frost et al., 2003; Pearson, 2004; Shetreat-Klein and Cropper, 2004; Buschges, 2005). The phasic, cycle-specific regulatory actions commonly result from direct synaptic actions on CPG neurons and associated motor neurons. In contrast, sensory activation or termination of CPG activity often results from its influences on upstream projection neurons.

Here, we use the stomatogastric nervous system (STNS) of the crab *Cancer borealis* to document that the same proprioceptor neuron can activate and regulate rhythmic motor activity, via distinct synaptic actions on different regions of the same projection neuron. The STNS includes four ganglia that contain a set of distinct but interacting CPGs controlling various aspects of the ingestion and processing of food by the foregut (Nusbaum and Beenhakker, 2002). The CPGs that generate the chewing (gastric mill circuit) and filtering (pyloric circuit) motor patterns occur in the stomatogastric ganglion (STG), while the projection neurons that regulate their activity are located primarily in the paired commissural (CoGs) ganglia. The gastric mill rhythm can be activated in the isolated STNS without sensory input (Coleman and Nusbaum, 1994), but sensory input does regulate this rhythm (Combes et al., 1999; Beenhakker et al., 2004; Blitz et al., 2004).

One well-defined sensory input to the gastric mill circuit is the gastro/pyloric receptors (GPRs), two pairs of bilaterally symmetric proprioceptor neurons that are activated by stretch of gastric mill protractor muscles (Katz et al., 1989; Katz and Harris-

Warrick, 1989). The GPRs modulate the pyloric rhythm and activate the gastric mill rhythm (Katz and Harris-Warrick, 1990; 1991; Blitz et al., 2004). They elicit the gastric mill rhythm by activating modulatory commissural neuron 1 (MCN1) and commissural projection neuron 2 (CPN2), which occur as single copies in each CoG (Blitz et al., 2004).

Blitz et al. (2004) studied the GPR ability to activate the gastric mill rhythm in an 'open-loop' paradigm in the isolated STNS wherein GPR was stimulated in a gastric mill-like pattern. Here we created a closed loop-like situation in the isolated STNS to understand how GPR influences an ongoing gastric mill rhythm activated by either a distinct sensory pathway or direct stimulation of MCN1 (Coleman and Nusbaum, 1994; Beenhakker et al., 2004). Specifically, during these rhythms, GPR was stimulated with a behaviorally-appropriate pattern, during each retractor phase, to close the GPR loop. With this approach, we demonstrate that GPR slows the gastric mill rhythm by selectively prolonging the retractor phase. This results from GPR-mediated presynaptic inhibition of the STG terminals of MCN1 and a parallel excitation of retractor phase neurons. The latter effect appears to enable GPR to replace a subset of the excitatory actions that it removes by its inhibition of MCN1.

Some of these results were published in abstract form (Beenhakker and Nusbaum, 2003).

METHODS

Animals/preparation. Male crabs, *Cancer borealis* (Jonah crabs), were obtained from Commercial Lobster & Seafood Co. (Boston, MA) and the Marine Biological Laboratory (Woods Hole, MA). Crabs were housed in commercial tanks containing chilled, filtered and recirculated artificial seawater (10°C). Before dissection, each crab was anesthetized by packing it in ice for at least 30 minutes. The foregut was removed and then transferred to a dissection dish containing saline (10-12°C) to enable dissection of the STNS from the foregut. The isolated STNS (Fig. 1*A*) was then transferred and pinned down in a silicone elastomer (Sylgard 184, KR Anderson, Santa Clara, CA)-lined Petri dish filled with saline (10-12°C).

Solutions. During dissection and experimentation, the STNS was supplied with *C. borealis* saline (mM): 440 NaCl, 26 $MgCl_2$, 11 KCl, 13 $CaCl_2$, 10 Trizma base and 5 maleic acid (pH 7.4-7.6). In some experiments, neuronal interactions were limited to those presumed to be monosynaptic by superfusing the preparation with saline containing 5 times the normal concentration of the divalent salts (high divalent cation saline) (Blitz and Nusbaum, 1999). This saline contained (in mM): 439 NaCl, 130 $MgCl_2$, 11 KCl, 64.5 $CaCl_2$, 10 Trizma base and 5 maleic acid (pH 7.4-7.6). During each experiment the STNS was continuously superfused with saline (7-12 ml/min), via a switching manifold to enable fast solution changes, and cooled (10-11°C) with a Peltier device.

Electrophysiology. STNS neurons were identified by their patterns of activity, synaptic interactions with other identified neurons and axonal branching patterns in connecting and peripheral nerves (Beenhakker et al., 2004; Beenhakker and Nusbaum, 2004).

Standard intracellular and extracellular recording techniques were used in this study (Beenhakker et al., 2004). Briefly, extracellular recordings of neuronal activity were obtained by electrically isolating individual sections of STNS nerves from the bath by building a petroleum jelly-based cylindrical compartment around a section of nerve. One of two stainless steel electrode wires was placed within this compartment, to record action potentials propagating through the nerve, while the second wire was placed in the bath as a reference electrode. The differential signal was recorded, filtered and amplified, first through an amplifier from AM Systems (Model 1700, Carlsborg, WA) and then through an amplifier from Brownlee Precision (Model 410, Santa Clara, CA). Extracellular stimulation of a nerve was achieved by placing the two extracellular wires into a stimulus isolation unit (Astromed/Grass Instruments, Model SIU5, West Warwick, RI) controlled by a stimulator (Astromed/Grass Instruments, Model S88). Intracellular recordings of STNS somata were obtained with sharp glass microelectrodes (15-30 MΩ) filled with either 4 M potassium acetate (KAc) plus 20 mM potassium chloride (KCl) or 0.6 M K_2SO_4 plus 20 mM KCl. Neurotransmitter release from the STG terminals of projection neurons is suppressed by intra-axonal recordings with KAc-filled electrodes positioned near the entrance to the STG (Coleman et al., 1995). Therefore, to preserve transmitter release during these intra-axonal recordings, we used an intracellular electrode solution of 1 M KCl (Bartos and Nusbaum, 1997). All intracellular signals were amplified and filtered with Axoclamp 2B amplifiers (Axon Instruments, Foster City, CA), and then further amplified with Brownlee Model 410 amplifiers. Intracellular current injections were performed in discontinuous current clamp (DCC) mode with sampling rates of 2-3 KHz.

In these experiments, we worked primarily with the GPR2 stretch receptor, by stimulating the *gpn* nerve through which its axon projects (Katz et al., 1989). However, we found that the STNS response to GPR1 stimulation was the same as GPR2 stimulation. The *gpn* also contains the axons of the lateral pyloric (LP) and medial gastric (MG) motor neurons (Katz et al., 1989). In general, GPR2 was selectively stimulated in our experiments, presumably because it has the largest diameter axon among these three neurons (Katz et al., 1989). Additionally, antidromically propagating action potentials in STG motor neurons only spread passively into the STG neuropil and therein only release transmitter when they occur on a sufficiently depolarized baseline (Mulloney and Selverston, 1972). In some of our experiments, the *gpn* was stimulated when the pyloric rhythm was suppressed (see Results). At these times, the membrane potentials of LP and MG were too hyperpolarized to enable antidromic spike-mediated transmitter release.

As GPR is activated during the retractor phase of the gastric mill rhythm (Katz and Harris-Warrick, 1989), we stimulated the *gpn* during this phase. This stimulation was performed manually by turning the stimulator on at the beginning of the retractor phase. We tested the effect of stimulating GPR for both a fixed duration and by terminating the stimulation at the burst onset time of the lateral gastric (LG) neuron. In the latter case, each stimulation was terminated either by anticipating the onset of the protractor phase (LG neuron burst onset), based on the trajectory of the LG neuron membrane potential, or else waiting until the start of each LG burst.

Data Acquisition. Data were acquired in parallel onto a chart recorder (MT-95000 or Everest Model, Astromed Corp., West Warwick, RI), and by digitizing (~5 KHz) and

storing the data on computer with data acquisition hardware/software (SPIKE2, Cambridge Electronic Design, Cambridge, England). Digitized data were analyzed with a homemade SPIKE2 program ('The Crab Analyzer', freely available at http://www.neurobiologie.de/). Briefly, the burst duration of a neuron was defined as the elapsed time (sec) between the first and last action potential in an impulse burst. The firing frequency was calculated by dividing the number of action potentials minus one by the burst duration. Gastric mill cycle period was defined by the duration (sec) between the onsets of 2 successive impulse bursts in the LG neuron.

Data are presented as mean ± SD. Statistical analyses were performed with SigmaStat 3.0 (SPSS, Chicago, IL). Figures were made from SPIKE2 files incorporated in the Adobe Photoshop (Adobe, San Jose, CA) and Powerpoint graphics programs (Microsoft, Seattle, WA).

Dynamic Clamp. We used the dynamic clamp technique (Sharp et al., 1993; Prinz et al., 2004) to inject an artificial ionic or synaptic current into the LG neuron. The dynamic clamp software uses intracellularly recorded membrane potentials (V_m) of biological neurons to calculate an artificial current (I_{dyn}) using a conductance ($g_{dyn}(t)$) that is numerically computed as well as a predetermined reversal potential (E_{rev}). The artificial current is computed in real time, updated in each time step (0.2 ms) according to the new values of recorded membrane potential and injected back into the biological neuron. The intrinsic currents are computed according to the equations below:

$$I_{dyn} = g_{dyn} m^p \cdot h^q \cdot (V_1 - E_{syn})$$

$$\tau_X(V_2)\frac{dX}{dt} = X_\infty(V_2) - X; \quad X = m, h$$

$$X_\infty(V) = \frac{1}{1 + \exp\left(\frac{V - V_X}{k_X}\right)}$$

$$\tau_X(V) = \tau_{X,Lo} + \frac{\tau_{X,Hi} - \tau_{X,Lo}}{1 + \exp\left(-\frac{V - V_X}{|k_X|}\right)}$$

where V_1 and V_2 both represent the membrane potential V_m. The synaptic currents are computed according to the same equations where V_1 represents V_{Post} and V_2 represents V_{Pre}. The values of parameters used by dynamic clamp in the above equations are given in Table 1.

In the dynamic clamp experiments involving the injection of the interneuron 1 (Int1) inhibitory synaptic current into the LG neuron, we used a model cell to represent Int1. This model cell included a passive leak current and Hodgkin-Huxley-like voltage-dependent inward and outward currents that underlie action potential generation. Consistent with the biological gastric mill circuit (Coleman et al., 1995; Bartos et al., 1999), the model Int1 was inhibited by the pyloric dilator (PD) and LG neurons, ongoing recordings of which were maintained in the biological preparation. The activity of the model Int1 was used to inject a simulated inhibitory current into the LG neuron to mimic the effect of increasing the inhibitory action of the biological Int1 (see Bartos et al., 1999).

In experiments in which the modulatory action of the MCN1 projection neuron on the LG neuron was mimicked with the dynamic clamp software, we used previously published parameters for the peptide-elicited, voltage-dependent current as

characterized in other STG neurons (Golowasch and Marder, 1992; Swensen and Marder, 2000, 2001). In the biological network, the modulatory input from MCN1 to LG decays during each LG burst (Coleman and Nusbaum, 1994; Coleman et al., 1995). To mimic this decay we added an inactivation component to the modeled current (see Table 1 and Results).

These experiments were performed using the version of the dynamic clamp software developed in the Nadim laboratory (available at http://stg.rutgers.edu/software) on a PC running Windows XP and a NI PCI-6070-E data acquisition board (National Instruments, Austin, TX). All intracellular recordings were performed in single-electrode discontinuous current clamp mode.

Gastric Mill Model. We constructed a computational model modified from an existing conductance-based model of the gastric mill circuit (Nadim et al., 1998). The previously published version modeled the LG, Int1, and MCN1 neurons as having multiple compartments separated by an axial resistance, with each compartment possessing intrinsic and/or synaptic conductances. We modified this model only by adding an additional single compartment cell, representing the GPR neuron, and several additional synaptic conductances (Table 2). All other parameters were unmodified from those previously published.

To model the GPR neuron, we added a single compartment cell with a passive leak current plus Hodgkin-Huxley-like voltage-dependent inward and outward currents to effect action potential generation. Consistent with physiological measurements (see Results), this model neuron made an inhibitory synaptic connection onto a distal compartment of the MCN1 axon terminals (t0 compartment: see Nadim et al., 1998), as

well as an excitatory connection onto the Int1 neurite compartment. To mimic the cumulative actions of repeated GPR stimulations, the GPR synapse onto MCN1 was modeled as a slow activating, slow deactivating current. The conductances and other parameters of these currents were chosen to mimic the behavior of the gastric mill circuit in the presence of GPR stimulation (Table 2). In these models we only incorporated each of these two synapses separately, because our aim was to assess their individual contributions to the observed GPR action on the gastric mill rhythm. Finally, to mimic more accurately the known mechanisms of gastric mill rhythm generation, we also added an excitatory synaptic connection between MCN1 and Int1 (Coleman et al., 1995).

Simulations were performed on a PC with Windows XP. We used the *Network* simulation software developed in the Nadim laboratory, which was run using the freely available CYGWIN Linux emulation software package. We used a 4th order Runge-Kutta numerical integration method with time steps of 0.05 and 0.01 ms. Results were visualized by plotting outputted data points using the freely available GNUPLOT software package.

RESULTS

GPR prolongs the retractor phase of the VCN-elicited gastric mill rhythm

The gastric mill rhythm is a two-phase motor pattern in which there is a rhythmic repeating alternation in impulse bursts between teeth protraction- and retraction-related neurons (Heinzel et al., 1993). There are eight different gastric mill neurons in *C. borealis*, half of which are active during protraction and half are active during retraction (Beenhakker and Nusbaum, 2004). In this paper, we use LG neuron activity to represent the protractor phase while the retractor phase is represented by the activity of the dorsal gastric (DG) neuron and/or Int1 (Fig. 1*B*). The reciprocally inhibitory neurons LG and Int1 comprise the core of the gastric mill CPG (Coleman et al., 1995; Bartos et al., 1999).

In situ, the GPRs are rhythmically activated during each retraction phase of the gastric mill rhythm. For GPR2, this activity pattern results from its dendrites being embedded in a protractor (gm9a) muscle that is stretched during each DG retractor neuron burst (Katz and Harris-Warrick, 1989) (Fig. 1*B*). The gastric mill rhythm is generally not spontaneously active in vitro, but it can be readily triggered by stimulation of known sensory pathways, including transient stimulation of the VCN mechanosensory neurons (Beenhakker et al., 2004). The VCNs are a bilateral population of approximately 60 sensory neurons located in the interior stomach lining of the cardiac sac (food storage) stomach compartment, near the entrance to the gastric mill. Application of adequate pressure to this location, or extracellular stimulation of the dorsal posterior oesophageal nerve (*dpon*), through which the VCN axons project to the CoGs, triggers a long-lasting gastric mill rhythm via VCN actions on CoG projection

neurons (see below) (Beenhakker et al., 2004; Beenhakker and Nusbaum, 2004). To determine what, if any, changes occurred in an ongoing gastric mill rhythm as a result of activating GPR at the behaviorally appropriate time, we stimulated GPR during successive DG neuron bursts in an ongoing VCN-elicited gastric mill rhythm (eg, Fig. 2).

There were three attractive features of using the VCN mechanosensory system to activate the gastric mill circuit. First, a relatively brief (1-2 min) stimulation of the VCNs triggers a long-lasting (tens of minutes) gastric mill rhythm (Beenhakker et al., 2004). Second, both the VCNs and the GPRs elicit the gastric mill rhythm via the same two CoG projection neurons, MCN1 and CPN2 (Beenhakker & Nusbaum, 2004; Blitz et al., 2004), thereby confining the scope of the pertinent circuitry to a limited number of neurons. The VCN- and GPR-elicited gastric mill rhythms are qualitatively similar but quantitatively distinct (Blitz et al., 2004). Third, the ability of the GPRs to influence MCN1 and CPN2 in the CoGs is suppressed during the VCN-elicited gastric mill rhythm, thereby limiting the likely locus of any persisting GPR actions to the STG (Beenhakker, 2004).

Stimulating GPR during each DG neuron burst slowed the gastric mill rhythm (Cycle Period: pre-GPR, 7.6 ± 1.8 sec; during GPR stim., 10.7 ± 3.4 sec; post-GPR, 8.2 ± 1.1 sec; Repeated Measures ANOVA: $p<0.001$, $n=8$) (Fig. 2). This slowing of the rhythm resulted from a selective increase in retractor phase duration that occurred during every cycle in which GPR was stimulated (Fig. 2*B*). For example, there was a consistent increase in the DG retractor neuron burst duration when GPR was stimulated (pre-GPR: 3.3 ± 1.8 sec; during GPR stim.: 6.6 ± 2.9 sec; post-GPR: 3.2 ± 0.5 sec; Repeated Measures ANOVA: $p<0.05$, $n=4$) (Fig 2*B*). In contrast, GPR stimulation did

not alter the duration of the LG protractor neuron (pre-GPR: 3.8 ± 1.1 sec; during GPR stim.: 4.2 ± 1.4 sec; post-GPR: 3.6 ± 1.0 sec; Repeated Measures ANOVA: $p>0.05$; n=8) (Fig. 2*B*). These GPR actions did not extend far past the final GPR stimulation. For example, DG neuron burst duration was prolonged for one additional cycle while gastric mill cycle period returned to pre-GPR levels as soon as GPR stimulation was terminated (Fig. 2*B*).

The selective increased duration of the gastric mill retractor phase by GPR stimulation also changed the relative fraction of each cycle (duty cycle) devoted to protraction and retraction. Specifically, GPR stimulation reduced the LG neuron duty cycle by causing a phase advance of its burst termination (pre-GPR: 49.6 ± 9%, during GPR stim.: 39.5 ± 9%, post-GPR: 43.3 ± 8%; pre-GPR vs. during GPR: $p<0.05$, n=8), and it increased the DG neuron duty cycle by phase advancing its burst onset (pre-GPR: 63.1 ± 9%, during GPR stim.: 49.7 ± 8%, post-GPR: 64.1 ± 8%; pre-GPR vs. during GPR: $p<0.05$, n=4). Thus, when GPR was active the gastric mill rhythm changed from having a balanced participation of the protractor and retractor neurons in each cycle to one in which there was relatively more retractor phase activity.

GPR prolongs the retractor phase by its synaptic actions in the STG

The GPR and VCN neurons both activate the gastric mill rhythm by eliciting a long-lasting activation of the projection neurons MCN1 and CPN2 (see Fig. 1) (Beenhakker and Nusbaum, 2004; Blitz et al., 2004). These two projection neurons appear to play distinct roles, with MCN1 providing the main excitatory drive to the gastric mill circuit while CPN2 sculpts the activity patterns of the gastric mill neurons

(Norris et al., 1994; Bartos et al., 1999; Beenhakker and Nusbaum, 2004). Surprisingly, during the VCN-elicited gastric mill rhythm, GPR stimulation no longer influences MCN1 or CPN2 in the CoGs as these GPR actions are effectively and reversibly masked by the VCN influence on these projection neurons (Beenhakker, 2004). It therefore appeared likely that the GPR ability to prolong selectively the retractor phase of the VCN-elicited gastric mill rhythm resulted from direct GPR actions within the STG.

We tested this hypothesis by transecting the superior- (*sons*) and inferior oesophageal nerves (*ions*) to eliminate the CoGs and assessing the influence of GPR stimulation on gastric mill rhythms elicited by selective extracellular nerve (*ion*) stimulation of MCN1 (Fig 3*A*). Under these conditions, tonic MCN1 stimulation routinely elicits the gastric mill rhythm (Bartos et al., 1999). Although two STG-projecting neurons, MCN1 and MCN5, project to the STG through the *ion* (Coleman and Nusbaum, 1994; Norris et al., 1996), low stimulus voltages selectively activate MCN1 (Bartos and Nusbaum, 1997; Bartos et al., 1999).

During MCN1-elicited gastric mill rhythms, GPR stimulation during the retractor phase again slowed the rhythm by selectively prolonging the retractor phase (Figs. 3*B*, 4). In fact, all of the GPR actions on the VCN-elicited gastric mill rhythm also occurred when GPR was rhythmically stimulated during the MCN1-elicited gastric mill rhythm with the CoGs removed. For example, these rhythmic GPR stimulations prolonged the gastric mill cycle period (pre-GPR: 5.6 ± 1 sec; during GPR: 9.0 ± 3 sec; post-GPR: 6.4 ± 1 sec; $p<0.05$, Repeated Measures ANOVA, n=6) (Fig. 4*A*) without changing the LG neuron burst duration (pre-GPR: 2.4 ± 0.9 sec; during GPR: 1.9 ± 0.3 sec; post-GPR: 2.4 ± 0.8 sec; $p>0.05$, Repeated Measures ANOVA, n=6) (Fig. 4*B*). Moreover, as

indicated for the VCN-elicited rhythm, by maintaining the same LG neuron burst duration while prolonging the gastric mill cycle period these GPR stimulations reduced LG neuron duty cycle (before GPR: 41.0 ± 11%; during GPR: 22.9 ± 9%; after GPR: 37.5 ± 11%; $p<0.01$, Repeated Measures ANOVA, n=6) (Fig. 4*C*).

GPR does not slow the gastric mill rhythm via its synapses on STG neurons

GPR has numerous synaptic actions within the STG on both gastric mill and pyloric neurons (Katz and Harris-Warrick, 1989, 1990, 1991; see below). Among the GPR targets are several pathways by which GPR could slow the gastric mill rhythm. The first of these pathways consists of the electrically-coupled pyloric pacemaker neurons (AB, PD neurons), whose rhythmic bursting activity is modulated by GPR (Katz and Harris-Warrick, 1990). The pyloric pacemaker neurons regulate the gastric mill cycle period via their rhythmic inhibition of Int1, which in turn provides pyloric-timed removal of Int1 inhibition (disinhibition) to the LG neuron (Nadim et al., 1998; Bartos et al., 1999). These disinhibitions, which are evident during each LG interburst (e.g., Fig. 3*B*), shorten the time to LG neuron burst onset after the preceding LG burst, thereby increasing the speed of the gastric mill rhythm (Bartos et al., 1999; Wood et al., 2004). Consequently, changing the frequency of these pyloric-timed disinhibitions causes a concomitant change in the speed of the gastric mill rhythm (Bartos et al., 1999). We tested and eliminated this pathway as the means by which GPR regulates the gastric mill cycle period by suppressing the pyloric pacemaker activity with hyperpolarizing current injection during an ongoing MCN1-elicited gastric mill rhythm. Despite the

absence of both the pyloric rhythm and the disinhibitions in the LG neuron, there was no change in the GPR ability to slow the ongoing gastric mill rhythm (n=4).

Another means by which GPR could influence the speed of the gastric mill rhythm is by its excitatory action on the DG neuron (Katz and Harris-Warrick, 1989; Kiehn and Harris-Warrick, 1992), because at high firing frequencies the DG neuron can inhibit the LG neuron. However, as was the case when the pyloric pacemaker neurons were silenced, suppression of DG neuron activity by hyperpolarizing current injection did not alter the GPR influence on the gastric mill rhythm (n=3).

A third potential target of GPR that could mediate the slowing of the gastric mill rhythm is the LG neuron. The level of LG neuron activity and its ability to escape from Int1-mediated inhibition is instrumental to gastric mill rhythm generation (Coleman et al., 1995; Bartos et al., 1999). Moreover, previous work showed that GPR stimulation produces an initial, apparently polysynaptic inhibitory response in the LG neuron, followed by an extended period of enhanced pyloric-timed subthreshold membrane potential oscillations (Katz and Harris-Warrick, 1991). We also noticed the latter response (see Fig. 5*A*). However, we observed no change in the LG neuron membrane potential when GPR was stimulated during either the VCN- or MCN1-elicited gastric mill rhythms. We nonetheless sought to identify the neuron(s) responsible for this previously documented inhibitory action of GPR on the LG neuron because such a neuron could mediate the ability of GPR to prolong the retractor phase (by delaying the protractor phase) and thereby increase the cycle period of ongoing gastric mill rhythms.

We tested the hypothesis that Int1 was responsible for the observed GPR influence on the LG neuron. As mentioned above, the LG neuron and Int1 constitute

the pair of reciprocally-inhibitory neurons at the core of the gastric mill CPG, and Int1 is responsible for the subthreshold, pyloric-timed membrane potential oscillations that occur in the LG neuron (Coleman et al., 1994; Bartos et al., 1999). We found that GPR did indeed consistently excite Int1, during which there was an increased hyperpolarization in the LG neuron (n=5) (Fig. 5*A1*). This GPR action appeared to be monosynaptic, because GPR action potentials elicited constant-latency excitatory postsynaptic potentials (EPSPs) in Int1 that persisted in the presence of high divalent cation saline (Fig. 5*A2*).

It was possible that GPR excitation of Int1 also explained the GPR-mediated prolongation of the retractor phase of the gastric mill rhythm. Specifically, if GPR enhanced Int1 activity during the gastric mill rhythm then this would likely strengthen Int1 inhibition of the LG neuron, thereby slowing the LG neuron escape from Int1 inhibition and prolonging the retractor phase. It was not possible to test directly this hypothesis by suppressing Int1 activity because its activity is necessary for gastric mill rhythm generation (Bartos et al., 1999). Therefore, as a first step, we determined whether GPR stimulation did indeed increase Int1 activity during the gastric mill rhythm. Surprisingly, GPR stimulation did not increase the Int1 firing frequency during either the VCN- or MCN1-elicited gastric mill rhythms (VCN rhythms: pre-GPR: 19.3 ± 1.4 Hz; during GPR: 19.6 ± 0.9 Hz; $p>0.05$, n=6) (MCN1 rhythms: pre-GPR: 17.6 ± 0.9 Hz; during-GPR: 19.1 ± 1.3 Hz; $p>0.05$, n=2) (Fig. 5*B*). Despite the lack of change in Int1 firing frequency during these GPR stimulations, the gastric mill rhythm was slowed as usual (n=8) (Fig. 5*B*).

There remained two possible mechanisms by which GPR excitation of Int1 could increase Int1 inhibition of the LG neuron. First, GPR might selectively enhance the graded component of Int1 transmitter release. STG circuit neurons exhibit both spike-mediated and graded release (Hartline and Graubard, 1992). The second possibility was that GPR could increase the amount of transmitter release per Int1 action potential.

We assessed the possibility that a GPR-mediated strengthening of the Int1 inhibition of the LG neuron was responsible for the GPR actions on the gastric mill rhythm in two ways. First, we implemented a modified version of our previously developed computational model of the MCN1-elicited gastric mill rhythm (Nadim et al., 1998; see Methods). Using this model, we found that when the Int1 inhibitory input to the LG neuron was strengthened by GPR excitation of Int1, the gastric mill rhythm was measurably slowed (cycle period: control, 11.2 ± 0.02 s; with GPR stimulation, 15.2 s) (Fig. 6). However, in contrast to the biological condition, both the retractor and protractor phases of these cycles were prolonged (protractor phase duration: control, 7.4 ± 0.02 s; with GPR stimulation, 9.7s; retractor phase duration: control, 3.7 ± 0.01 s; with GPR stimulation, 7.8 s).

To understand the consequences of increasing the strength of Int1 inhibition of the LG neuron, it is helpful to know the previously documented interactions between MCN1, Int1 and LG. Specifically, each LG neuron burst initiates after a period during which it steadily depolarizes to escape from Int1-mediated inhibition, due to the buildup of excitatory drive that LG receives from MCN1 during this phase of the rhythm (Coleman et al., 1995; Bartos et al., 1999) (Fig. 6). Thus, when Int1 inhibition of LG was strengthened, the LG neuron required more time to build up more excitatory drive from

MCN1 to enable it to escape from Int1 inhibition. When the LG burst finally was initiated, it inhibited the STG terminals of MCN1 (as well as Int1) (Coleman and Nusbaum, 1994; Coleman et al., 1995), causing the excitatory drive it had received from MCN1 to decay.

The strengthened Int1 inhibition of LG thus caused an increased LG neuron burst duration for the following reason. The excitatory drive from MCN1 not only mediates LG escape from Int1 inhibition but it is responsible for the LG neuron burst. Specifically, the LG neuron has no intrinsic ability to generate a prolonged burst without synaptic input such as that from MCN1 (Coleman and Nusbaum, 1994; Bartos et al., 1999). Consequently, when the duration of a constant level of MCN1 input is prolonged, as it was to enable the LG neuron to escape from the strengthened Int1 inhibition, it built up more excitatory drive in LG. Because the level of excitatory drive at the time of burst onset was higher than in the control rhythm, and the rate of decay from MCN1 excitation was unchanged by strengthening Int1 input, the time needed for this increased level of modulatory drive to decay to the LG burst termination point was prolonged (Fig. 6).

To test the predictions of this model, we returned to the biological system and used the dynamic clamp technique to inject an additional Int1-like inhibitory conductance into LG during each Int1 period of activity (i.e., during the time when GPR would be active) (see Methods for details; see also Bartos et al., 1999). As a result of this increased inhibitory conductance, there was an increased hyperpolarization in the LG neuron (by –7.8 ± 1.2 mV; n=6). LG nonetheless remained able to escape the combined biological and dynamic clamp-mediated inhibition, and the gastric mill rhythm was maintained (Fig. 7). Under these conditions, the retractor phase was reversibly

prolonged (pre-DClamp: 5.6 ± 1.8 sec; DClamp: 12.1 ± 4.7 sec; post-DClamp: 6.9 ± 1.5 sec; Two-way ANOVA $p<0.01$; Tukey pairwise comparison: DClamp vs. Pre. $p<0.01$, DClamp vs. Post, $p<0.05$, Post vs. Pre, $p>0.05$; n=6) as was the gastric mill cycle period (pre-DClamp: 9.7 ± 2.5 sec; DClamp: 18.3 ± 6.0 sec; post-DClamp: 11.2 ± 2.0 sec; Two-way ANOVA $p<0.005$; Tukey pairwise comparison: DClamp vs. Pre, $p<0.005$, DClamp vs. Post, $p<0.05$, Post vs. Pre, $p>0.05$; n=6) (Fig. 7*A*,*B*). Additionally, as predicted by the modeling results, the LG (protractor phase) neuron burst duration was also reversibly prolonged (pre-DClamp: 4.1 ± 1.2 sec; DClamp: 6.2 ± 2.6 sec; post-DClamp: 4.3 ± 1.5 sec; Two-way ANOVA $p<0.005$; Tukey pairwise comparison: DClamp vs. Pre, $p<0.005$, DClamp vs. Post, $p<0.01$, Post vs. Pre, $p>0.05$; n=6) (Fig. 7*A,B*). These results, combined with the fact that GPR stimulation did not change the Int1 firing frequency during the gastric mill rhythm, led us to conclude that the GPR-mediated selective prolongation of the gastric mill retractor phase and associated slowing of the rhythm was not likely to result, at least exclusively, from its excitation of Int1.

GPR stimulation inhibits the STG terminals of MCN1

We next examined the possibility that the GPR ability to prolong selectively the gastric mill retractor phase resulted from GPR inhibition of the STG terminals of MCN1. Depending on its strength, such a synaptic action would slow or prevent the LG neuron escape from Int1 inhibition. MCN1 drive to the gastric mill circuit, including its slow excitation of the LG neuron, occurs primarily during each retractor phase because its transmitter release is reduced by presynaptic inhibition from the LG neuron during each protractor phase (Coleman and Nusbaum, 1994; Coleman et al., 1995). We therefore

tested the hypothesis that the GPR-mediated prolongation of the retractor phase and the associated slowing of the gastric mill rhythm resulted from GPR inhibition of the STG terminals of MCN1. To this end, we recorded intra-axonally from MCN1 in the stomatogastric nerve (*stn*: $MCN1_{stn}$), near the entrance to the STG (see Fig. 8*A*). This recording site is electrotonically close to the MCN1 terminals in the STG ($MCN1_{STG}$), and electrotonically distant from its arborization and spike initiation zone in the CoG ($MCN1_{CoG}$) (Coleman and Nusbaum, 1994).

GPR stimulation consistently evoked a hyperpolarizing response in $MCN1_{stn}$ (n=5) (Fig. 8*B*). This hyperpolarization was graded in amplitude, correlated with the frequency of GPR stimulation (data not shown). Unlike the LG-mediated presynaptic inhibition of MCN1 (Coleman and Nusbaum, 1994), however, we did not record any unitary IPSPs in $MCN1_{stn}$ in response to GPR stimulation. Instead the GPR-mediated inhibition exhibited a relatively slow rise and decay, taking several seconds to repolarize after GPR stimulation was terminated (Fig. 8*B*). This inhibitory action was likely to occur within the STG neuropil, from where it spread passively to the $MCN1_{stn}$ recording site, as is the case for the LG inhibition of $MCN1_{STG}$ (Coleman and Nusbaum, 1994). This expectation was based on the fact that the GPR-mediated hyperpolarization neither suppressed nor reduced in amplitude or duration the *ion*-elicited action potentials recorded at $MCN1_{stn}$. Instead, as also occurs during LG inhibition of $MCN1_{STG}$ (Coleman and Nusbaum, 1994), these action potentials were either unchanged or increased slightly in amplitude. A comparable increase in the amplitude of *ion*-elicited action potentials occurred at $MCN1_{stn}$ when the MCN1 axon was comparably hyperpolarized by current injection (data not shown).

We could not assess the functional consequences of the GPR-mediated presynaptic inhibition of MCN1 by using an STG target of MCN1 as a reporter neuron, as we did in characterizing the LG presynaptic inhibition of MCN1 (Coleman and Nusbaum, 1994). This was because every STG target of MCN1 was also a direct and/or indirect target of GPR (Katz and Harris-Warrick, 1990, 1991; this paper). Therefore, we instead used several alternative means to assess the impact of the GPR inhibition on MCN1 transmitter release within the STG. First, to determine more directly whether this GPR-mediated inhibition could effectively influence $MCN1_{STG}$ activity, we took advantage of the fact that injecting depolarizing current into $MCN1_{\textit{stn}}$ evokes action potentials that are initiated within the STG neuropil (Coleman and Nusbaum, 1994). Consequently, we assessed how GPR stimulation affected MCN1 spike initiation within the STG. To this end, we either injected tonic depolarizing current to elicit tonic MCN1 activity, or else repeatedly (1 Hz) injected 100 msec duration depolarizing current pulses into $MCN1_{\textit{stn}}$ such that each control pulse elicited several MCN1 action potentials. During tonic $MCN1_{STG}$ stimulation, GPR stimulation reversibly suppressed MCN1 activity (n=3). During rhythmic $MCN1_{STG}$ depolarizations, GPR stimulation consistently and reversibly reduced the number of MCN1 action potentials produced during each depolarizing pulse (pre-GPR: 3.9 ± 0.1 spikes; during GPR: 1.6 ± 1.1 spikes; post-GPR: 3.5 ± 0.1 spikes, $p<0.05$; n=2) (Fig. 9).

Although GPR stimulation effectively inhibited the spike-initiating ability of $MCN1_{STG}$, the GPR influence on incoming MCN1 action potentials was more complex. Specifically, when MCN1 action potentials propagated through the *stn* into the STG during the GPR-mediated hyperpolarization, the electrical EPSPs from MCN1 to LG

persisted (not shown). This result left unresolved the issue of whether the GPR inhibition of $MCN1_{STG}$ was ineffective at regulating the influence of MCN1 or, as in the case of the LG inhibition of $MCN1_{STG}$ (Coleman and Nusbaum, 1994; Coleman et al., 1995), this GPR-mediated inhibition affected MCN1 transmitter release without suppressing the electrical synapses made by MCN1.

To address this issue, we returned to our computational model of the gastric mill system and assessed therein the consequences of GPR inhibition of $MCN1_{STG}$ (see Table 2). As shown in Figure 10, this model predicted that within a given range of inhibitory conductances the GPR inhibition of $MCN1_{STG}$ could mimic the actions of GPR on the biological gastric mill rhythm. Specifically, within this conductance range, GPR inhibition of $MCN1_{STG}$ selectively prolonged the gastric mill retractor phase and thereby slowed the rhythm. However, when inhibitory conductances larger than this range were used, LG could not escape from Int1 inhibition and the gastric mill rhythm was terminated.

The results from the model supported the hypothesis that the GPR ability to prolong selectively the gastric mill retractor phase involved the reduction but not elimination of MCN1 transmitter release. This is evident in Figure 10 from the reduced but persisting MCN1 modulation in the LG neuron during GPR stimulation. In this version of the model, we maintained the same level of Int1 inhibition of LG during the rhythm with and without GPR stimulation, to reflect the unchanged Int1 activity level during GPR stimulation in the physiological situation (Fig. 5*B*). If MCN1 transmitter release was eliminated, the LG neuron would not have been able to escape from Int1 inhibition as long as GPR activity continued. However, when the GPR inhibition of

$MCN1_{STG}$ only reduced MCN1 excitation of LG (peak synaptic conductance during GPR ~50% of control peak), then the retractor phase of the model rhythm was prolonged. This extended retractor phase occurred because it took more time to build up the same level of excitatory drive in LG that normally occurs in the absence of GPR activity, which is the amount needed by LG to escape a constant level of Int1 inhibition and generate a burst (Fig. 10). Once that level was attained, the LG neuron fired its burst, inhibiting MCN1 and thereby starting the down-regulation of its own activity. Unlike the situation in which Int1 inhibition of LG was strengthened (Figs. 6, 7), here the same amount of excitatory drive from MCN1 was attained by LG at the time of its burst onset. Thus, the modulatory effect decayed with the same time course as occurred before GPR stimulation, leaving the LG burst duration unchanged.

We then assessed whether the outcomes of the model were likely to reflect the related biological events by using two approaches. First, we tested the model prediction that the rate at which the MCN1 excitation of the LG neuron developed during the retractor phase selectively regulates the retractor phase duration. We did this by tonically stimulating MCN1 at different frequencies and assessing the resulting duration of the retractor and protractor phases. As shown qualitatively by Bartos et al. (1999), the MCN1 firing frequency determines the speed of the gastric mill rhythm primarily by its control of the retractor phase duration. Our quantitative analysis showed that this is indeed the case. Specifically, the gastric mill cycle period consistently decreased as MCN1 firing frequency increased (Cycle period: MCN1 (6-7 Hz), 14.5 ± 5.3 sec; MCN1 (10 Hz), 10.7 ± 3.5 sec; MCN1 (15 Hz), 9.4 ± 2.7 sec; MCN1 (20 Hz), 7.7 ± 1.9 sec; Two-way ANOVA $p<0.005$; $n=7$). This change in cycle period was due largely to the

parallel change in retractor phase duration (Retractor Phase Duration: MCN1 (6-7 Hz), 9.7 ± 4.8 sec; MCN1 (10 Hz), 5.7 ± 2.4 sec; MCN1 (15 Hz), 3.6 ± 1.2 sec; MCN1 (20 Hz), 3.0 ± 1.0 sec; Two-way ANOVA $p<0.005$; $n=7$). Under these conditions, the protractor phase duration was unchanged (Protractor Phase Duration: MCN1 (6-7 Hz), 4.8 ± 1.9 sec; MCN1 (10 Hz), 5.0 ± 2.0 sec; MCN1 (15 Hz), 5.8 ± 2.2 sec; MCN1 (20 Hz), 4.7 ± 1.5 sec; Two-way ANOVA, $p>0.05$; $n=7$).

Second, we used the dynamic clamp to generate a gastric mill-like rhythm by selectively introducing, and manipulating, the likely MCN1-mediated conductance into the LG neuron. For this purpose, we used the peptide-activated current that was first characterized in the *C. borealis* STG to mediate the actions of the peptide proctolin on the pyloric circuit (Golowasch and Marder, 1992) (see Methods). This current, termed the "proctolin current", was subsequently shown to mediate also the actions of other neuroactive peptides on the pyloric circuit in *C. borealis* (Swensen and Marder, 2000, 2001). One of these peptides is CabTRP Ia, which is the peptide transmitter used by MCN1 to excite the LG neuron (Wood et al., 2000).

For these experiments we used preparations in which the STG remained in communication with the CoGs, to ensure a relatively high rate of spontaneous activity in Int1. As commonly occurs in the isolated STNS, Int1 exhibited spontaneous, pyloric-timed activity while the LG neuron was silent (Bartos et al., 1999). Injection of a sufficient level of the proctolin conductance into the LG neuron (see Table 1) enabled LG to escape from Int1 inhibition and fire action potentials. To terminate each LG burst and thereby mimic the gastric mill rhythm-related burst pattern of LG, we added a slow inactivation variable to the proctolin current to mimic the LG presynaptic inhibition of

MCN1 that normally regulates that current (Coleman and Nusbaum, 1994; see Methods) (Fig. 11). Consequently, the proctolin current was effectively increasing in amplitude during each LG interburst and decaying during each LG burst.

We then implemented different rates of increase for this modulatory current in order to determine whether this rate could selectively regulate the duration of the retractor phase. To this end, we compared gastric mill-like rhythms with relatively slow (tau=160-320s) and fast (tau=8-16s) rates of rise for this excitatory drive. Consistent with the model predictions, the relatively slowly developing dynamic clamp excitation of LG caused a slower rhythm (cycle period: fast rise, 10.97 ± 4.4s; slow rise, 18.49 ± 5.2s; t-test, $p<0.005$, n=5) with a selectively prolonged retractor phase relative to the faster developing excitation (retractor phase duration: fast rise, 6.62 ± 2.7s; slow rise, 14.19 ± 4.3s; t-test, $p<0.005$, n=5; protractor phase duration: fast rise, 4.36 ± 2.1s; slow rise, 4.30 ± 1.0s; t-test, $p>0.05$, n=5) (Fig. 11). These results thus support the hypothesis that the selective prolongation of the retractor phase by GPR stimulation can result from its presynaptic inhibition of $MCN1_{STG}$ slowing the buildup of modulatory excitation from MCN1 to LG during the retractor phase.

DISCUSSION

Sensory inputs shape rhythmic motor activity via direct and indirect actions on the underlying CPG (Pearson, 2004; Buschges, 2005). Although the significance of these inputs to rhythmic motor activity is well documented, the mechanisms through which sensory actions reshape motor output have not been elucidated in most systems. Here we show that the phasically-activated muscle stretch receptor neuron GPR regulates the gastric mill rhythm at least partly by presynaptically inhibiting the modulatory projection neuron MCN1 (Fig. 12). In parallel, GPR postsynaptically excites the retractor phase neurons Int1 and DG (Katz and Harris-Warrick, 1989; this paper) (Fig, 12). The presynaptic inhibition reduces the excitatory drive from MCN1 to all gastric mill neurons, while the postsynaptic excitation appears to function as a replacement for the reduced drive from MCN1 to the retractor neurons. The consequence for the gastric mill rhythm is a selectively prolonged retractor phase and slower cycle period.

GPR regulation of the gastric mill system via presynaptic inhibition of a modulatory projection neuron represents a novel mechanism for phasic sensory regulation of ongoing motor activity. Most previous studies of phasic sensory regulation have instead highlighted CPG and motor neurons as the sensory neuron targets (Hooper and Moulins, 1990; Katz and Harris-Warrick, 1990, 1991; Buschges and el Manira, 1998; Rosen et al., 2000; Shetreat-Klein and Cropper, 2004; Pearson, 2004; Buschges, 2005). However, rhythmic stimulation of the anterior gastric receptor (AGR), a muscle tendon receptor in the lobster STNS, does reconfigure an ongoing gastric mill rhythm via synaptic actions in the CoGs on projection neurons (Combes et al., 1999).

Sensory regulation of neural circuit activity

To optimize the understanding of how sensory systems influence their targets by manipulating them in the isolated CNS, it is important to implement the biologically appropriate activity pattern for that sensory system. This experimental approach has led to an improved understanding, albeit not yet at the level of identified circuit neurons, of phasic sensory influence on both intra- and inter-limb coordination during locomotion (Pearson, 2004; Buschges, 2005). We therefore recapitulated a behaviorally-relevant scenario for the GPR neurons by replicating their previously documented response to stretch of the muscles in which their dendrites are embedded (Katz et al., 1989; Birmingham et al., 1999). Our approach is likely to approximate events occurring in the feeding animal because the VCN neurons are thought to be activated during stomach distention (Beenhakker et al., 2004), and the VCN-triggered chewing motor pattern would involve rhythmic stretch of the GPR-innervated muscles. Under some conditions, however, GPR exhibits either a modest activation during the protractor phase or is spontaneously rhythmic (Katz et al., 1989; Birmingham et al., 1999). We did not study these situations, but our results suggest that GPR activation during the protractor phase would have at most a small impact on the gastric mill rhythm because at this time MCN1 receives strong presynaptic inhibition from LG (Coleman and Nusbaum, 1994).

Acute activation of the GPR neurons when there is no gastric mill rhythm evokes a reflex response that includes a relatively long-lasting activation of gastric mill retractor neurons and a modulation of the pyloric rhythm (Katz and Harris-Warrick, 1989, 1990, 1991). The gastric mill response is a reinforcing reflex because activation of the

retractor neuron DG stretches the muscle in which the GPR dendrites are embedded, and GPR in turn evokes a burst of activity in DG (Katz and Harris-Warrick, 1989; Kiehn and Harris-Warrick, 1992). During the gastric mill rhythm, the prolonged reflex response is eventually terminated because the LG neuron escapes from Int1 inhibition and terminates retractor neuron activity (Coleman et al., 1995; this paper).

The GPR effect of prolonging the retractor phase of the gastric mill rhythm is not achieved by directly or indirectly increasing the level of synaptic inhibition in the protractor CPG neuron LG. As elucidated by our computer model and supported by our dynamic clamp experiments, prolonging the retractor phase via any synaptic influence on the LG neuron increases the duration of the subsequent LG burst, contrary to the GPR actions on the gastric mill rhythm. Thus, to prolong selectively the retractor phase, GPR instead reduces the MCN1 influence on the entire gastric mill circuit to delay the onset of the next protractor phase and, in parallel, helps maintain the retractor phase by substituting its own excitatory drive to the retractor neurons.

It may seem surprising that GPR stimulation did not increase the level of Int1 activity during the gastric mill rhythm, given its ability to excite directly Int1. However, although we did not test directly the effectiveness of this synaptic action during the gastric mill rhythm, GPR is likely to use this synapse to compensate for the reduced MCN1 excitation of Int1 that results from GPR inhibition of $MCN1_{STG}$. Drawing the conclusion that GPR excitation of Int1 was responsible for the ability of GPR to delay the onset of the protractor phase would have been reasonable given the key role played by the Int1 inhibition of LG in gastric mill rhythm generation (Coleman et al., 1995; Bartos et al., 1999). The fact that this synapse was not pivotal for the GPR-mediated

selective prolongation of the retractor phase provides a valuable lesson in understanding circuit operation. If we had not examined the GPR effect on Int1 activity during the gastric mill rhythm and had not considered the consequences of changing Int1 activity in terms of the buildup of MCN1 excitation of the LG neuron, we might not have searched for GPR influences on $MCN1_{STG}$.

Regulation of circuit activity at multiple sites on the same projection neuron

There are not many systems where it has been possible to document the presence and function of spatially separate synaptic actions by a single neuron onto the same target neuron. Our work with GPR illustrates such an example in that GPR causes a long-lasting excitation of $MCN1_{CoG}$ and a shorter-lasting inhibition of $MCN1_{STG}$ (Blitz et al., 2004; this paper) (Fig. 12). GPR also excites CPN2 in the CoGs, and its co-activation of these two projection neurons initiates the gastric mill rhythm (Blitz et al., 2004). When GPR stimulation elicits the gastric mill rhythm, it also appears to be effectively inhibiting $MCN1_{STG}$ because this version of the gastric mill rhythm is slower than that elicited by the VCN mechanosensory neurons, due to a prolonged retractor phase (Blitz et al., 2004). It will be instructive to determine whether the opposing GPR actions on $MCN1_{CoG}$ and $MCN1_{STG}$ are mediated by the same or different GPR cotransmitters, which include acetylcholine, serotonin and the peptide allatostatin (Katz and Harris-Warrick, 1989; Skiebe and Schneider, 1994).

The excitatory actions of GPR on MCN1 and CPN2 in the CoG are state-dependent, in that they are absent when these projection neurons have been recently activated by the VCNs (Beenhakker, 2004). This state-dependent excitation of

$MCN1_{CoG}$ and $CPN2_{CoG}$ by GPR facilitates the ability of GPR to slow this rhythm via its actions in the STG. Specifically, if GPR continued to excite $MCN1_{CoG}$ during the VCN-elicited gastric mill rhythm, then the increased MCN1 firing frequency would likely result in a reduced effectiveness of the GPR inhibition of $MCN1_{STG}$.

Presynaptic inhibition enables sensory signals to dynamically regulate neural circuit activity

The role of presynaptic inhibition in the context of sensorimotor integration is commonly discussed with regard to the gating in or, more commonly, gating out of sensory information (Nusbaum et al., 1997; Buschges and el Manira, 1998; Evans et al., 2003; Katz, 2004). One frequently documented example of this gating mechanism is the primary afferent depolarization that occurs on sensory axon terminals to reduce sensory input to CPG networks. This has been particularly well-studied for presynaptic inhibition of sensory input to the locomotor network of both vertebrates and invertebrates (Buschges and el Manira, 1998; Rudomin and Schmidt, 1999; Cattaert et al., 2001; Frost et al., 2003). This presynaptic inhibition can be regulated in a spinal segment-specific manner (Lomeli et al., 1998; Rudomin et al., 2004). Presynaptic inhibition of projection neuron terminals also occurs at reticulospinal axon terminals relevant to lamprey swimming, but its role in motor pattern generation remains to be elucidated (Svensson et al., 2003). The findings described herein extend these studies by showing that proprioceptor-mediated presynaptic inhibition of a modulatory projection neuron can contribute to phase-specific regulation of rhythmic activity.

The parallel presynaptic and postsynaptic actions of the GPR proprioceptor neuron enable it to mediate simultaneously its reflex function of prolonging teeth retraction without terminating ongoing CPG activity. If GPR instead terminated CPG activity to mediate its reflex function, then once GPR activity ceased it would take several gastric mill cycles until the rhythm was back to its steady-state level (Bartos et al., 1999). Instead, as shown here, the gastric mill rhythm returns to its pre-GPR activity level as soon as GPR activity terminates.

Another level of control in this system is suggested by the fact that the sensitivity of GPR to muscle stretch is itself modulated (Birmingham, 2001; Birmingham et al., 2003). We therefore anticipate that our appreciation for how sensory signals regulate neural circuit activity will be extended further as we assess the consequences resulting from modulation of GPR sensitivity for its influence on the gastric mill motor circuit.

REFERENCES

Bartos M, Nusbaum MP (1997) Intercircuit control of motor pattern modulation by presynaptic inhibition. J Neurosci 17:2247-2256.

Bartos M, Manor Y, Nadim F, Marder E, Nusbaum MP (1999) Coordination of fast and slow rhythmic neuronal circuits. J Neurosci 19:6650-6660.

Beenhakker MP (2004) Sensory regulation of rhythmically active neuronal networks. PhD Thesis, University of Pennsylvania.

Beenhakker MP, Nusbaum MP (2003) Sensory regulation of a modulatory projection neuron at two separate locations. Soc Neurosci Abstr 60411.

Beenhakker MP, Nusbaum MP (2004) Mechanosensory activation of a motor circuit by coactivation of two projection neurons. J Neurosci 24: 6741-6750.

Beenhakker MP, Blitz DM, Nusbaum MP (2004) Long-lasting activation of rhythmic neuronal activity by a novel mechanosensory system in the crustacean stomatogastric nervous system. J Neurophysiol 91:78-91.

Birmingham JT (2001) Increasing sensor flexibility through neuromodulation. Biol Bull 200:206-210.

Birmingham JT, Szuts Z, Abbott LF, Marder E (1999) Encoding of muscle movement on two time scales by a sensory neuron that switches between spiking and burst modes. J Neurophysiol 82:2786-2797.

Birmingham JT, Billimoria CP, De Klotz TR, Stewart RA, Marder E (2003) Differential and history-dependent modulation of a stretch receptor in the stomatogastric system of the crab, *Cancer borealis*. J Neurophysiol 90:3608-3616.

Blitz DM, Beenhakker MP, Nusbaum MP (2004) Different sensory systems share projection neurons but elicit distinct motor patterns. J Neurosci 24: 11381-11390.

Blitz DM, Nusbaum MP (1999) Distinct functions for cotransmitters mediating motor pattern selection. J Neurosci 19:6774-6783.

Buschges A (2005) Sensory control and organization of neural networks mediating coordination of multisegmental organs for locomotion. J Neurophysiol 93:1127-1135.

Buschges A, el Manira AE (1998) Sensory pathways and their modulation in the control of locomotion. Curr Opin Neurobiol 8:733-739.

Cattaert D, Libersat F, El Manira A (2001) Presynaptic inhibition and antidromic spikes in primary afferents of the crayfish: a computational and experimental analysis. J Neurosci 21:1007-1021.

Coleman MJ, Nusbaum MP (1994) Functional consequences of compartmentalization of synaptic input. J Neurosci 14:6544-6552.

Coleman MJ, Meyrand P, Nusbaum MP (1995) A switch between two modes of synaptic transmission mediated by presynaptic inhibition. Nature 378:502-505.

Combes D, Meyrand P, Simmers J (1999) Dynamic restructuring of a rhythmic motor program by a single mechanoreceptor neuron in lobster. J Neurosci 19:3620-3628.

Di Prisco GV, Pearlstein E, Le Ray D, Robitaille R, Dubuc R (2000) A cellular mechanism for the transformation of a sensory input into a motor command. J Neurosci 21:8169-8176.

Evans CG, Jing J, Rosen SC, Cropper EC (2003) Regulation of spike initiation and propagation in an *Aplysia* sensory neuron: gating-in via central depolarization. J Neurosci 23:2920-2931.

Frost WN, Tian L-M, Hoppe TA, Mongeluzi DL, Wang J (2003) A cellular mechanism for prepulse inhibition. Neuron 40:991-1001.

Golowasch J, Marder E (1992) Proctolin activates an inward current whose voltage dependence is modified by extracellular Ca^{2+}. J Neurosci 12:810-817.

Hartline DK, Graubard K (1992) Cellular and synaptic properties in the crustacean stomatogastric nervous system. In: Dynamic Biological Networks: The Stomatogastric Nervous System (Harris-Warrick RM, Marder E, Selverston AI, Moulins M, eds), pp 31-86. Cambridge, MA: MIT Press.

Heinzel H-G, Weimann JM, Marder E (1993) The behavioral repertoire of the gastric mill in the crab, *Cancer pagurus*: an in situ endoscopic and electrophysiological examination. J Neurosci 13:1793-1803.

Hooper SL, Moulins M (1990) Cellular and synaptic mechanisms responsible for a long-lasting restructuring of the lobster pyloric network. J Neurophysiol 64: 1574-1589.

Katz PS (2004) Synaptic gating: the potential to open closed doors. Curr Biol 13:R554-R5565.

Katz PS, Eigg MH, Harris-Warrick RM (1989) Serotonergic/cholinergic muscle receptor cells in the crab stomatogastric nervous system. I. Identification and characterization of the gastropyloric receptor cells. J Neurophysiol 62:558-570.

Katz PS, Harris-Warrick RM (1989) Serotonergic/cholinergic muscle receptor cells in the crab stomatogastric nervous system. II. Rapid nicotinic and prolonged

modulatory effects on neurons in the stomatogastric ganglion. J Neurophysiol 62:571-581.

Katz PS, Harris-Warrick RM (1990) Neuromodulation of the crab pyloric central pattern generator by serotonergic/cholinergic proprioceptive afferents. J Neurosci 10:1495-1512.

Katz PS, Harris-Warrick RM (1991) Recruitment of crab gastric mill neurons into the pyloric motor pattern by mechanosensory afferent stimulation. J Neurophysiol 65:1442-1451.

Kiehn O, Harris-Warrick RM (1992) Serotonergic stretch receptors induce plateau properties in a crustacean motor neuron by a dual-conductance mechanism. J Neurophysiol 68:485-495.

Lomeli J, Quevedo J, Linares P, Rudomin P (1998) Local control of information flow in segmental and ascending collaterals of single afferents. Nature 395:600-604.

McCrea DA (1998) Neuronal basis of afferent-evoked enhancement of locomotor activity. Ann N Y Acad Sci 860:216-225.

Mulloney B, Selverston A (1972) Antidromic action potentials fail to demonstrate known interactions between neurons. Science 177:69-72.

Nadim F, Manor Y, Nusbaum MP, Marder E (1998) Frequency regulation of a slow rhythm by a fast periodic input. J Neurosci 18:5053-5067.

Norris BJ, Coleman MJ, Nusbaum MP (1994) Recruitment of a projection neuron determines gastric mill motor pattern selection in the stomatogastric nervous system of the crab, *Cancer borealis*. J Neurophysiol. 72:1451-1463.

Norris BJ, Coleman MJ, Nusbaum MP (1996) Pyloric motor pattern modification by a newly identified projection neuron in the crab stomatogastric nervous system. J Neurophysiol. 75:97-108.

Nusbaum MP, Beenhakker MP (2002) A small-systems approach to motor pattern generation. Nature 417:343-350.

Nusbaum MP, El Manira A, Gossard J-P, Rossignol S (1997) Presynaptic mechanisms during rhythmic activity in vertebrates and intervebrates. In: Neurons, Networks and Motor Behavior (Stein PSG, Grillner S, Selverston A, Stuart DG, eds), pp 237-253. Cambridge, MA: MIT Press.

Pearson K (2004) Generating the walking gait: role of sensory feedback. Prog Brain Res 143:123-129.

Perrins R, Walford A, Roberts A (2002) Sensory activation and role of inhibitory reticulospinal neurons that stop swimming in hatchling frog tadpoles. J Neurosci 22:4229-4240.

Prinz AA, Abbott LF, Marder E (2004) The dynamic clamp comes of age. Trends Neurosci 27:218-224.

Rosen SC, Miller MW, Evans CG, Cropper EC, Kupfermann I (2000) Diverse synaptic connections between peptidergic mechanoafferent neurons and neurons in the feeding system of *Aplysia*. J Neurophysiol 83:1605-1620.

Rudomin P, Lomeli J, Quevedo J (2004) Differential modulation of primary afferent depolarization of segmental and ascending intraspinal collaterals of single muscle afferents in the cat spinal cord. Exp Brain Res 156:377-391.

Rudomin P, Schmidt RF (1999) Presynaptic inhibition in the vertebrate spinal cord revisited. Exp Brain Res 129:1-37.

Sharp AA, O'Neil MB, Abbott LF, Marder E (1993) The dynamic clamp: artificial conductances in biological neurons. Trends Neurosci. 16:389-394.

Shetreat-Klein AN, Cropper EC (2004) Afferent-induced changes in rhythmic motor programs in the feeding circuitry of *Aplysia*. J Neurophysiol 92:2312-2322.

Skiebe P, Schneider H (1994) Allatostatin peptides in the crab stomatogastric nervous system: inhibition of the pyloric motor pattern and distribution of allatostatin-like immunoreactivity. J Exp Biol 194:195-208.

Stein PSG, Grillner S, Selverston AI, Stuart DG, eds (1997) Neurons, networks, and motor behavior. Cambridge, MA: The MIT Press.

Svensson E, Wikstrom MA, Hill RH, Grillner S (2003) Endogenous and exogenous dopamine presynaptically inhibits glutamatergic reticulospinal transmission via an action of D2-receptors on N-type Ca2+ channels. Eur J Neurosci 17:447-454.

Swensen AM, Marder E (2000) Multiple peptides converge to activate the same voltage-dependent current in a central pattern-generating circuit. J Neurosci 20:6752-6759.

Swensen AM, Marder E (2001) Modulators with convergent cellular actions elicit distinct circuit outputs. J Neurosci. 21:4050-4058.

Wood DE, Manor Y, Nadim F, Nusbaum MP (2004) Intercircuit control via rhythmic regulation of projection neuron activity. J Neurosci 25: 7455-7463.

Wood DE, Stein W, Nusbaum MP (2000) Projection neurons with shared cotransmitters elicit different motor patterns from the same neural circuit. J Neurosci 20:8943-

8953.

Table 1. Parameters used in dynamic clamp experiments.

Table 2. Parameters used to incorporate GPR synapses into an existing model of the gastric mill rhythm (Nadim et al., 1998). GPR was modeled as a single compartment cell with active and passive properties, and three synaptic currents were added to existing model cells. “Inst” denotes an instantaneous time constant.

Figure 1. Schematic of the isolated stomatogastric nervous system (STNS) and the pathways by which two identified sensory systems influence the gastric mill circuit. ***A,*** The STNS consists of the unpaired stomatogastric (STG) and oesophageal (OG) ganglia, the paired commissural (CoG) ganglia, plus the connecting and peripheral nerves. In each CoG there is a single a copy of each identified CoG projection neuron, including MCN1, MCN5, MCN7 and CPN2. The STNS receives sensory information from the proprioceptor neurons GPR1 and 2, and the mechanoreceptor VCNs. ***B,*** The GPRs and VCNs each elicit the gastric mill rhythm by activating MCN1 and CPN2, which in turn activate the gastric mill circuit. The gastric mill CPG neurons LG and Int1 have reciprocal inhibitory connections and are influenced by the pyloric pacemaker neuron AB. The dorsal gastric (DG) neuron is a gastric mill retractor motor neuron that innervates the gm4 muscle. Contraction of gm4 stretches the GPR-innervated muscles, thereby activating the GPRs (Katz and Harris-Warrick, 1989). Synapse symbols: t-bars, excitation; filled circles, inhibition; resistor, electrical coupling. **Abbreviations. Nerves**: *dgn*, dorsal gastric nerve; *dpon*, dorsal posterior oesophageal nerve; *ion*, inferior

oesophageal nerve; *lgn*, lateral gastric nerve; *lvn*, lateral ventricular nerve; *mgn*, medial gastric nerve; *mvn*, medial ventricular nerve; *son*, superior oesophageal nerve; *stn*, stomatogastric nerve; *vcn*, ventral cardiac nerve. **Neurons**: AB, anterior burster; CPN2, commissural projection neuron 2; GPR, gastropyloric receptor; MCN1,5,7, modulatory projection neuron 1,5,7; VCN, ventral cardiac neuron.

Figure 2. GPR stimulation prolongs the retractor phase of the VCN-elicited gastric mill rhythm. ***A,*** Stimulating GPR (5 Hz intraburst frequency) in a behaviorally-relevant pattern during the VCN-elicited gastric mill rhythm in the isolated stomatogastric nervous system slows the rhythm by selectively prolonging the retractor phase. ***B,*** Relative to pre-GPR stimulation levels, during each cycle when GPR was stimulated (arrows) there was a significant increase in the duration of the gastric mill retractor phase and in the duration of the cycle period, but there was no change in the protractor phase duration (*$p<0.05$; $n=8$; One Way Repeated Measures ANOVA, Student-Newman Keuls Test). Each bar represents a single gastric mill cycle, with one cycle shown pre-, 5 cycles during- and 4 cycles post-GPR stimulation. Note the rapid return to control levels after GPR stimulation was terminated.

Figure 3. Influence of GPR on the MCN1-elicited gastric mill rhythm. ***A,*** Preparation used to study the MCN1-elicited gastric mill rhythm. The CoGs were eliminated by transection of the *ions* and *sons*, and selective MCN1 stimulation was accomplished by extracellular stimulation of the *ion* to elicit the gastric mill rhythm (Bartos et al., 1999). ***B,*** Stimulating GPR during the retractor phase of the MCN1-elicited gastric mill rhythm

selectively prolonged that retractor phase. MCN1 stimulation (black bar: 30 Hz tonic) began before the presented recording segment and persisted for the duration of the recording shown. Most hyperpolarized Vm: LG, -75 mV.

Figure 4. Quantification of the GPR actions on the MCN1-elicited gastric mill rhythm. The pre- (white bars), during- (black bars) and post-GPR stimulation (gray bars) conditions each represent the mean of 5 consecutive gastric mill cycles. ***A,*** GPR stimulation during the MCN1-elicited gastric mill rhythm reversibly prolonged the gastric mill cycle period by ~60% ($p<0.05$, $n=6$). ***B/C,*** Stimulating GPR during the MCN1-elicited gastric mill rhythm (B) did not alter the LG neuron burst duration ($p>0.05$, $n=6$) but (C) reduced the fraction of a gastric mill cycle during which LG was active (LG duty cycle) by nearly 20% ($p<0.01$, $n=6$).

Figure 5. GPR excites Int1 but does not alter Int1 activity during the gastric mill rhythm. ***A1,*** In the isolated STG with no ongoing gastric mill rhythm, GPR stimulation (5 Hz) excited Int1 and produced a concomitant increase in the amplitude of the subthreshold, pyloric-timed oscillations in the LG neuron. ***A2,*** Single GPR stimuli evoked constant latency EPSPs in Int1 in high divalent cation saline. EPSP represents the average of 8 Int1 responses to GPR stimulation. The relatively long latency to EPSP onset results from the ~2 cm distance traveled by the GPR-elicited action potentials to reach the STG. ***B1,*** GPR stimulation (5 Hz) during an ongoing MCN1-elicited gastric mill rhythm prolonged the retractor phase without an evident change in Int1 activity. ***B2,*** GPR failed to enhance Int1 activity during ongoing gastric mill rhythms at times when it did prolong

the gastric mill cycle period. Shown are the mean (±SD) gastric mill cycle period (white symbols) and corresponding Int1 firing frequency (gray symbols) before and during GPR stimulation for 8 preparations, organized by symbol shape. The dotted line represents no change between the pre- and during-GPR conditions. ***B3,*** Int1 firing frequency (black bars) and gastric mill cycle period (white bars) data are normalized to pre-control conditions. In the same preparations, GPR stimulation increased the gastric mill cycle period (40.8 ± 28.9%; $p<0.001$, n=8) but failed to alter Int1 firing frequency (4.5 ± 5.4%; $p>0.05$; n=8).

Figure 6. Increasing the strength of Int1 inhibition of the LG neuron during GPR stimulation prolongs both phases of the MCN1-elicited gastric mill rhythm in a computational model. GPR was stimulated during a retractor phase, as occurs in the biological system. In this version of the model, the strength of Int1 inhibition of LG was explicitly enhanced by GPR stimulation. The result was an increase in the duration of that retractor phase (Int1 active) as well as an increase in the subsequent protractor phase (LG active). Note that the rhythm returned to control levels in the next cycle. The modulatory current (I_{Mod}) trace represents the cycle-by-cycle buildup and decay of MCN1 excitation of the LG neuron. When GPR is silent, the LG neuron burst initiates when the level of modulatory current attains the level designated as “normal LG burst threshold”. Most hyperpolarized Vm: Int1, -65 mV; LG, -55 mV.

Figure 7. Increasing the strength of Int1 inhibition of the LG neuron with the dynamic clamp, in the biological preparation, slows the gastric mill rhythm by prolonging both

phases of the rhythm. ***A,*** During an ongoing MCN1-elicited gastric mill rhythm, the dynamic clamp was used to increase the strength of Int1 inhibition of the LG neuron. This increased inhibition led to a prolonged retractor phase as well as a longer duration of each subsequent protractor phase. The vertical lines occurring periodically during the LG burst (rising above and below the action potentials) and interburst represent artifacts that occur when recording in discontinuous current clamp-mode while performing nerve (*ion*) stimulation. ***B,*** Quantitative analysis supporting the result represented in Panel *A*. Under these conditions, GPR stimulation reversibly prolonged the LG burst duration, LG interburst duration and gastric mill cycle period ($p<0.01$, $n=6$).

Figure 8. GPR stimulation hyperpolarizes the STG terminals of MCN1. ***A,*** Schematic of the isolated STNS (left), with an expanded view of the STG (right) to indicate the location of the intra-axonal recording site for $MCN1_{stn}$. ***B,*** Intracellular recording of $MCN1_{stn}$ revealed a hyperpolarizing response to GPR stimulation (5 Hz). Note the subthreshold pyloric-timed oscillations in $MCN1_{stn}$. The thickened $MCN1_{stn}$ trace during GPR stimulation represents the stimulus artifact.

Figure 9. GPR stimulation inhibits MCN1 action potential initiation within the STG neuropil. ***A,*** Injecting depolarizing current into $MCN1_{stn}$ initiates action potentials within the STG neuropil (Coleman and Nusbaum, 1994). Constant duration (100 msec) and amplitude (+2nA) depolarizing pulses injected into $MCN1_{stn}$ produced a regular number (3-4) of action potentials/pulse. This number was reversibly reduced during GPR stimulation (5 Hz). Note the delay of several seconds after GPR stimulation before the

number of MCN1 action potentials/pulse returns to control levels. ***B,*** Expanded traces from panel *A* of single pulses (1) before, (2) during and (3) after GPR stimulation.

Figure 10. The GPR action on the MCN1-elicited gastric mill rhythm is best mimicked by GPR inhibition of $MCN1_{STG}$ in a computational model of the MCN1-elicited gastric mill rhythm. In this version of the model, GPR stimulation presynaptically inhibited $MCN1_{STG}$, thereby reducing MCN1 actions onto the LG neuron. As a result, the amplitude of the modulatory current (I_{Mod}) induced in LG by MCN1 is reduced during GPR stimulation. This effect persists after GPR stimulation due to the slow time constant of the GPR action. The GPR inhibition of $MCN1_{STG}$ slowed the LG escape from Int1 inhibition, prolonging the retractor phase. Note that, in contrast, the protractor phase duration was not altered. Most hyperpolarized Vm: Int1, -65 mV; LG, -55 mV.

Figure 11. The rate of rise of MCN1-like modulation of the LG neuron selectively regulates the retractor phase duration. ***A,*** In this experiment, in place of MCN1 stimulation, the biological LG neuron was injected with a dynamic clamp version of the modulatory current that likely represents the current provided by MCN1 (Swensen and Marder, 2000; see Methods). The only parameter that differed during the dynamic clamp current injection in the two traces shown was the rate of rise of the current amplitude during each LG interburst. Note that the slower rate of rise (bottom trace) caused a slower rhythm, which resulted largely from a selectively prolonged LG interburst (retractor-like phase). Both LG traces are from the same preparation. ***B,*** Injecting the dynamic clamp version of the modulatory current into LG with a relatively

long time constant for its rise in amplitude consistently elicited gastric mill-like activity in LG that was slower, due to a selective increase in LG interburst duration, than that resulting from injection of the same current with a briefer time constant ($p<0.005$, $n=5$).

Figure 12. Working model of the GPR actions on the gastric mill system. Gastric mill-like rhythmic GPR stimulation can elicit the gastric mill rhythm (Blitz et al., 2004) by exciting the projection neuron MCN1 (and CPN2) in the commissural ganglia. During the gastric mill rhythm elicited by MCN1 (either directly or via activation of the VCN mechanosensory neurons), stimulating GPR in a behaviorally-appropriate manner (during each retractor DG neuron burst) slows the gastric mill rhythm by selectively prolonging the retractor phase. This latter GPR action results from GPR inhibition of the axon terminals of MCN1 in the stomatogastric ganglion, in concert with its excitation of the retractor neurons Int1 and DG. Synapse symbols: t-bars, excitation; filled circles, inhibition.

Table 1 – Dynamic Clamp Parameters

Synapses

Current	Vm (mV)	Km (mV)	TmLo (ms)	TmHi (ms)	P	Vh (mV)	Kh (mV)	ThLo (ms)	ThHi (ms)	Q	Gmax (nS)	Erev (mV)
LG-Int1	-45	-0.1	5	1500	1	n/a	n/a	n/a	n/a	0	30	-120
Int1-LG	-40	-1	5	200	1	n/a	n/a	n/a	n/a	0	100	-80
PD-Int1	-20	-1	5	1000	1	n/a	n/a	n/a	n/a	0	10	-120

Int1 Model Cell Currents

	Vm	Km	TmLo	TmHi	P	Vh	Kh	ThLo	ThHi	Q	Gmax	Erev
Leak	-40	-5	50	100	0	n/a	n/a	n/a	n/a	0	1	-60
Na	-40	-10	5	5	1	-40	3.0	50	50	1	30	45
K	-40	-10	100	500	1	n/a	n/a	n/a	n/a	0	50	-80

Simulated CabTRP Current in LG

	Vm	Km	TmLo	TmHi	P	Vh	Kh	ThLo	ThHi	Q	Gmax	Erev
CabTRP	-40	-10	200	50	1	-40	0.5	12000	8000	1	250	0

Table 2 – Model Parameters

Synapses

Synapse	Gmax (nS)	Erev (mV)	Minf	Mtau
MCN1-Int1	6	0	$\frac{1}{1+e^{-45(V+70)}}$	1
GPR-Int1	20	0	$\frac{1}{1+e^{-(V+60)}}$	50
GPR-MCN1	40	-80	$\frac{1}{1+e^{-(V+60)}}$	$2000+\frac{4000}{1+e^{V+60}}$

GPR Intrinsic Currents

Current	Gmax	Erev	p	q	Minf	Mtau	Hinf	Htau
Leak	3	-68	n/a	n/a	n/a	n/a	n/a	n/a
Na	120	50	3	1	$\frac{1}{1+e^{-5(V+62)}}$	Inst	$\frac{1}{1+e^{5(V+64)}}$	$1+\frac{5}{1+e^{-0.24(V+64)}}$
K	36	-77.5	4	n/a	$\frac{1}{1+e^{-5(V+54)}}$	$8+\frac{20}{1+e^{0.24(V+54)}}$	n/a	n/a

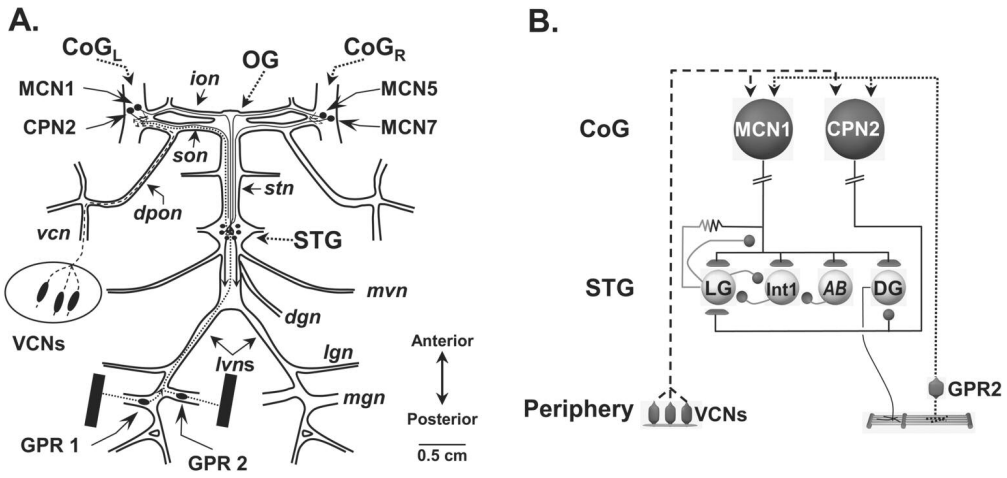

Figure 1. Schematic of the isolated stomatogastric nervous system (STNS) and the pathways by which two identified sensory systems influence the gastric mill circuit. A, The STNS consists of the unpaired stomatogastric (STG) and oesophageal (OG) ganglia, the paired commissural (CoG) ganglia, plus the connecting and peripheral nerves. In each CoG there is a single a copy of each identified CoG projection neuron, including MCN1, MCN5, MCN7 and CPN2. The STNS receives sensory information from the proprioceptor neurons GPR1 and 2, and the mechanoreceptor VCNs. B, The GPRs and VCNs each elicit the gastric mill rhythm by activating MCN1 and CPN2, which in turn activate the gastric mill circuit. The gastric mill CPG neurons LG and Int1 have reciprocal inhibitory connections and are influenced by the pyloric pacemaker neuron AB. The dorsal gastric (DG) neuron is a gastric mill retractor motor neuron that innervates the gm4 muscle. Contraction of gm4 stretches the GPR-innervated muscles, thereby activating the GPRs (Katz and Harris-Warrick, 1989). Synapse symbols: t-bars, excitation; filled circles, inhibition; resistor, electrical coupling. Abbreviations. Nerves: dgn, dorsal gastric nerve; dpon, dorsal posterior oesophageal nerve; ion, inferior oesophageal nerve; lgn, lateral gastric nerve; lvn, lateral ventricular nerve; mgn, medial gastric nerve; mvn, medial ventricular nerve; son, superior oesophageal nerve; stn, stomatogastric nerve; vcn, ventral cardiac nerve. Neurons: AB, anterior burster; CPN2, commissural projection neuron 2; GPR, gastropyloric receptor; MCN1,5,7, modulatory projection neuron 1,5,7; VCN, ventral cardiac neuron.
129x60mm (300 x 300 DPI)

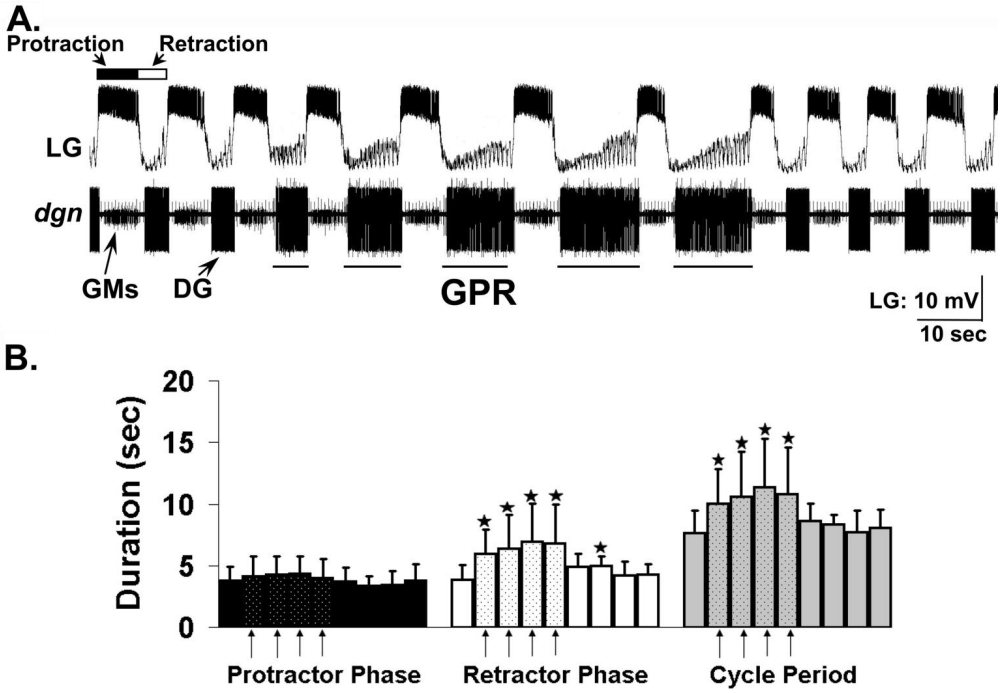

Figure 2. GPR stimulation prolongs the retractor phase of the VCN-elicited gastric mill rhythm. A, Stimulating GPR (5 Hz intraburst frequency) in a behaviorally-relevant pattern during the VCN-elicited gastric mill rhythm in the isolated stomatogastric nervous system slows the rhythm by selectively prolonging the retractor phase. B, Relative to pre-GPR stimulation levels, during each cycle when GPR was stimulated (arrows) there was a significant increase in the duration of the gastric mill retractor phase and in the duration of the cycle period, but there was no change in the protractor phase duration (*p<0.05; n=8; One Way Repeated Measures ANOVA, Student-Newman Keuls Test). Each bar represents a single gastric mill cycle, with one cycle shown pre-, 5 cycles during- and 4 cycles post-GPR stimulation. Note the rapid return to control levels after GPR stimulation was terminated.

129x89mm (300 x 300 DPI)

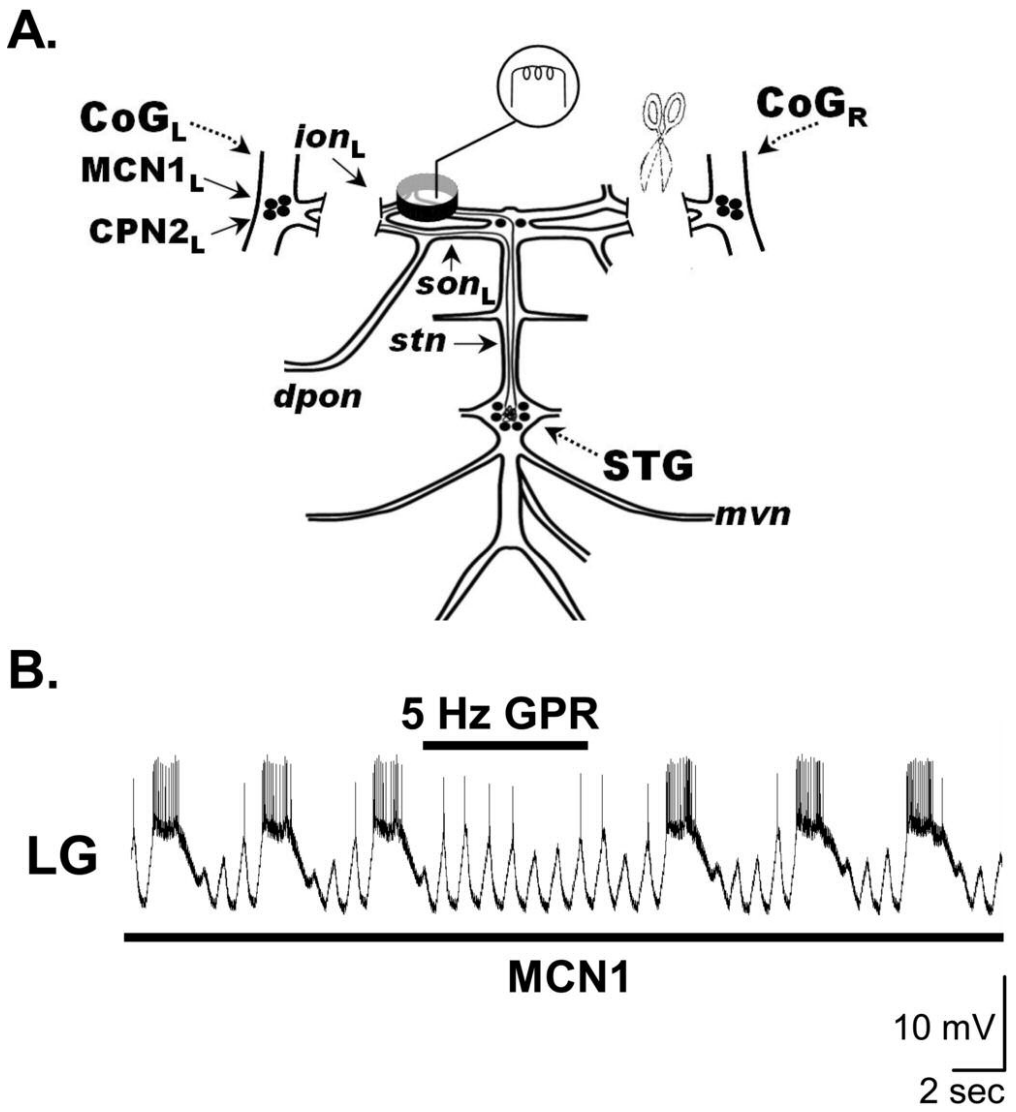

Figure 3. Influence of GPR on the MCN1-elicited gastric mill rhythm. A, Preparation used to study the MCN1-elicited gastric mill rhythm. The CoGs were eliminated by transection of the ions and sons, and selective MCN1 stimulation was accomplished by extracellular stimulation of the ion to elicit the gastric mill rhythm (Bartos et al., 1999). B, Stimulating GPR during the retractor phase of the MCN1-elicited gastric mill rhythm selectively prolonged that retractor phase. MCN1 stimulation (black bar: 30 Hz tonic) began before the presented recording segment and persisted for the duration of the recording shown. Most hyperpolarized Vm: LG, -75 mV.
87x96mm (300 x 300 DPI)

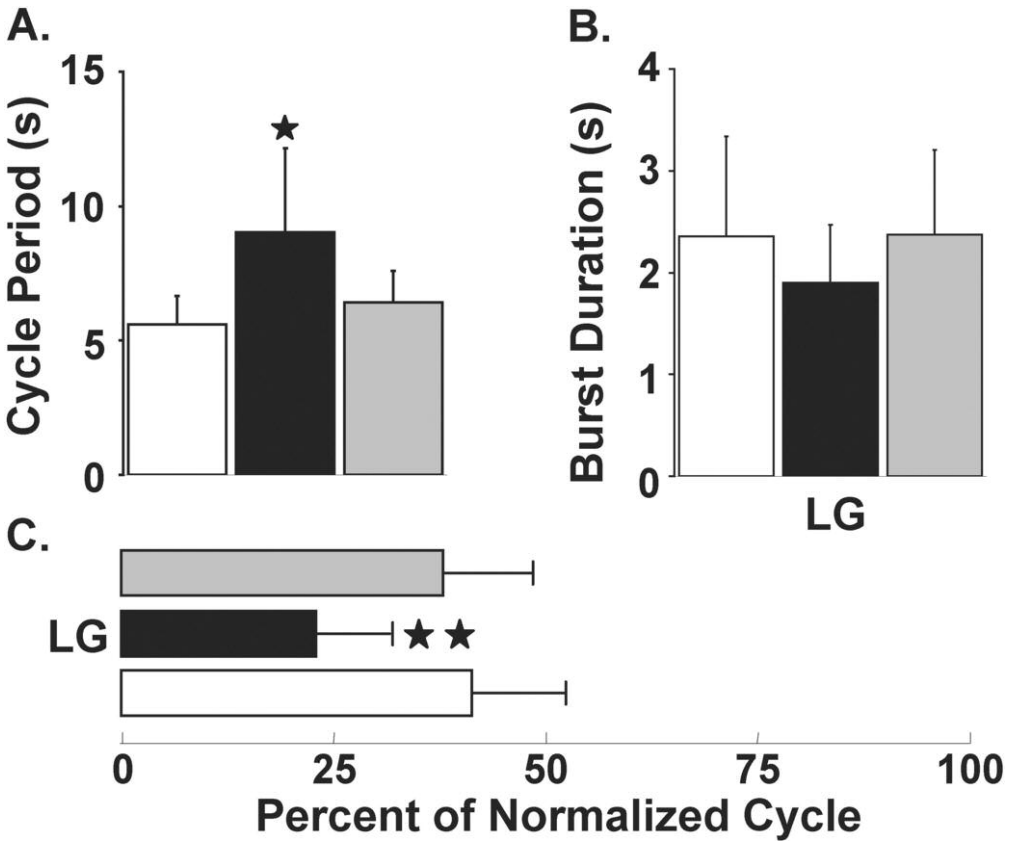

Figure 4. Quantification of the GPR actions on the MCN1-elicited gastric mill rhythm. The pre- (white bars), during- (black bars) and post-GPR stimulation (gray bars) conditions each represent the mean of 5 consecutive gastric mill cycles. A, GPR stimulation during the MCN1-elicited gastric mill rhythm reversibly prolonged the gastric mill cycle period by ~60% ($p<0.05$, $n=6$). B/C, Stimulating GPR during the MCN1-elicited gastric mill rhythm (B) did not alter the LG neuron burst duration ($p>0.05$, $n=6$) but (C) reduced the fraction of a gastric mill cycle during which LG was active (LG duty cycle) by nearly 20% ($p<0.01$, $n=6$).

87x73mm (300 x 300 DPI)

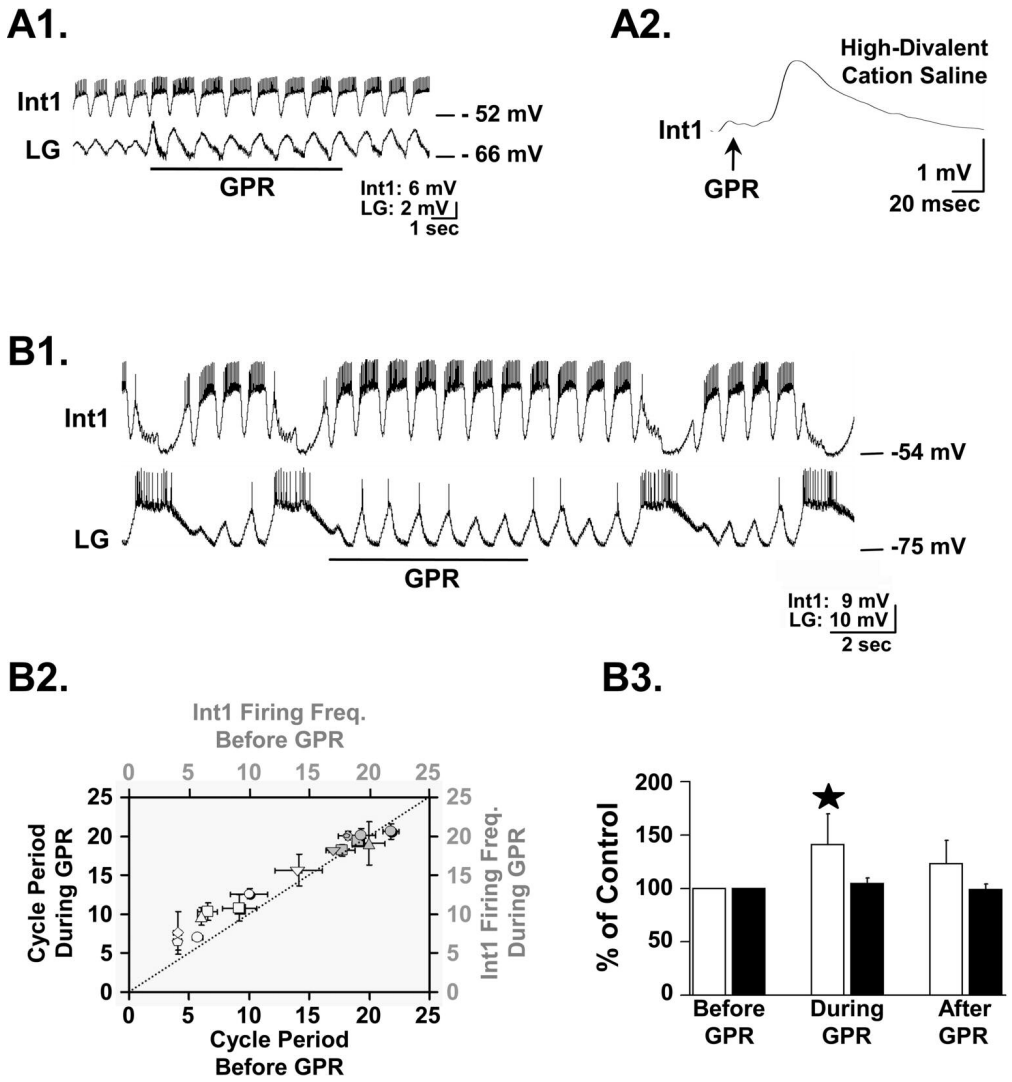

Figure 5. GPR excites Int1 but does not alter Int1 activity during the gastric mill rhythm. A1, In the isolated STG with no ongoing gastric mill rhythm, GPR stimulation (5 Hz) excited Int1 and produced a concomitant increase in the amplitude of the subthreshold, pyloric-timed oscillations in the LG neuron. A2, Single GPR stimuli evoked constant latency EPSPs in Int1 in high divalent cation saline. EPSP represents the average of 8 Int1 responses to GPR stimulation. The relatively long latency to EPSP onset results from the ~2 cm distance traveled by the GPR-elicited action potentials to reach the STG. B1, GPR stimulation (5 Hz) during an ongoing MCN1-elicited gastric mill rhythm prolonged the retractor phase without an evident change in Int1 activity. B2, GPR failed to enhance Int1 activity during ongoing gastric mill rhythms at times when it did prolong the gastric mill cycle period. Shown are the mean (±SD) gastric mill cycle period (white symbols) and corresponding Int1 firing frequency (gray symbols) before and during GPR stimulation for 8 preparations, organized by symbol shape. The dotted line represents no change between the pre- and during-GPR conditions. B3, Int1 firing frequency (black bars) and gastric mill cycle period (white bars) data are normalized to pre-control conditions. In the

same preparations, GPR stimulation increased the gastric mill cycle period (40.8 ± 28.9%; p<0.001, n=8) but failed to alter Int1 firing frequency (4.5 ± 5.4%; p>0.05; n=8).
129x138mm (300 x 300 DPI)

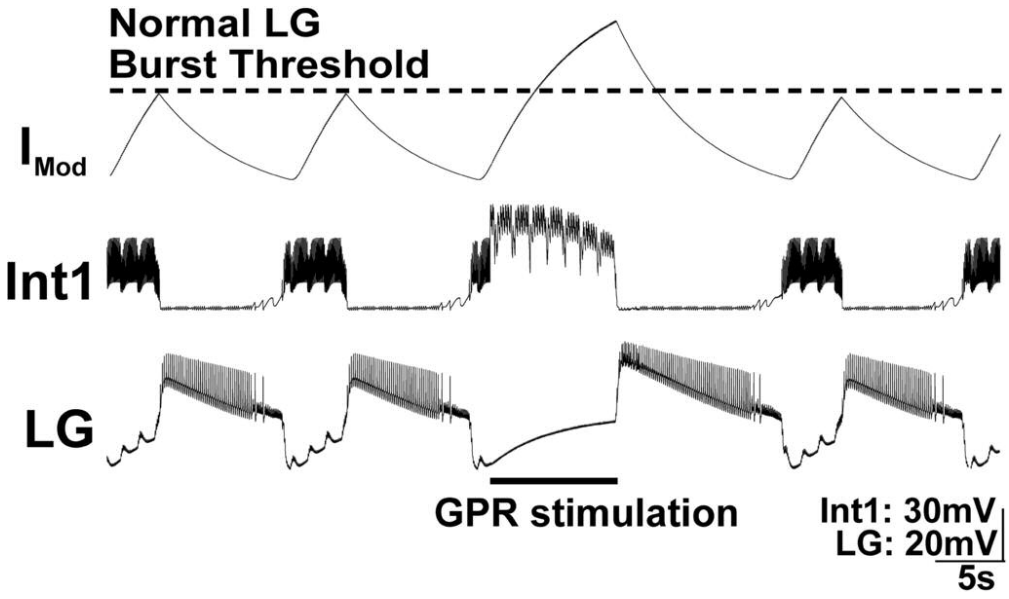

Figure 6. Increasing the strength of Int1 inhibition of the LG neuron during GPR stimulation prolongs both phases of the MCN1-elicited gastric mill rhythm in a computational model. GPR was stimulated during a retractor phase, as occurs in the biological system. In this version of the model, the strength of Int1 inhibition of LG was explicitly enhanced by GPR stimulation. The result was an increase in the duration of that retractor phase (Int1 active) as well as an increase in the subsequent protractor phase (LG active). Note that the rhythm returned to control levels in the next cycle. The modulatory current (IMod) trace represents the cycle-by-cycle buildup and decay of MCN1 excitation of the LG neuron. When GPR is silent, the LG neuron burst initiates when the level of modulatory current attains the level designated as □normal LG burst threshold□. Most hyperpolarized Vm: Int1, -65 mV; LG, -55 mV.
86x50mm (300 x 300 DPI)

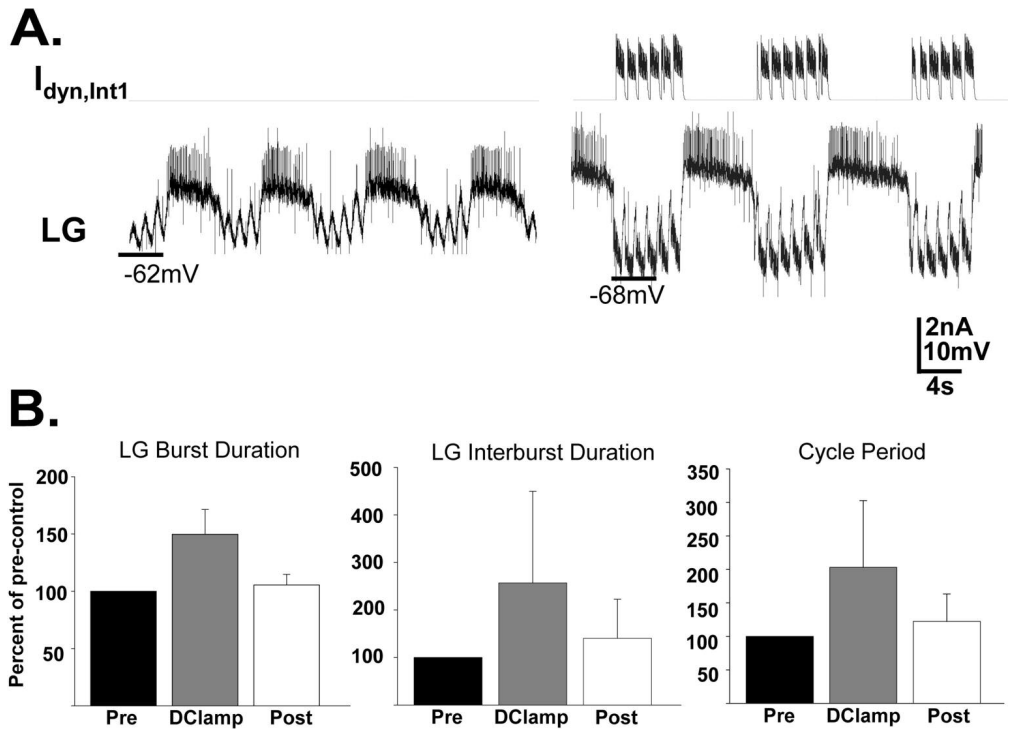

Figure 7. Increasing the strength of Int1 inhibition of the LG neuron with the dynamic clamp, in the biological preparation, slows the gastric mill rhythm by prolonging both phases of the rhythm. A, During an ongoing MCN1-elicited gastric mill rhythm, the dynamic clamp was used to increase the strength of Int1 inhibition of the LG neuron. This increased inhibition led to a prolonged retractor phase as well as a longer duration of each subsequent protractor phase. The vertical lines occurring periodically during the LG burst (rising above and below the action potentials) and interburst represent artifacts that occur when recording in discontinuous current clamp-mode while performing nerve (ion) stimulation. B, Quantitative analysis supporting the result represented in Panel A. Under these conditions, GPR stimulation reversibly prolonged the LG burst duration, LG interburst duration and gastric mill cycle period ($p<0.01$, $n=6$).
129x93mm (300 x 300 DPI)

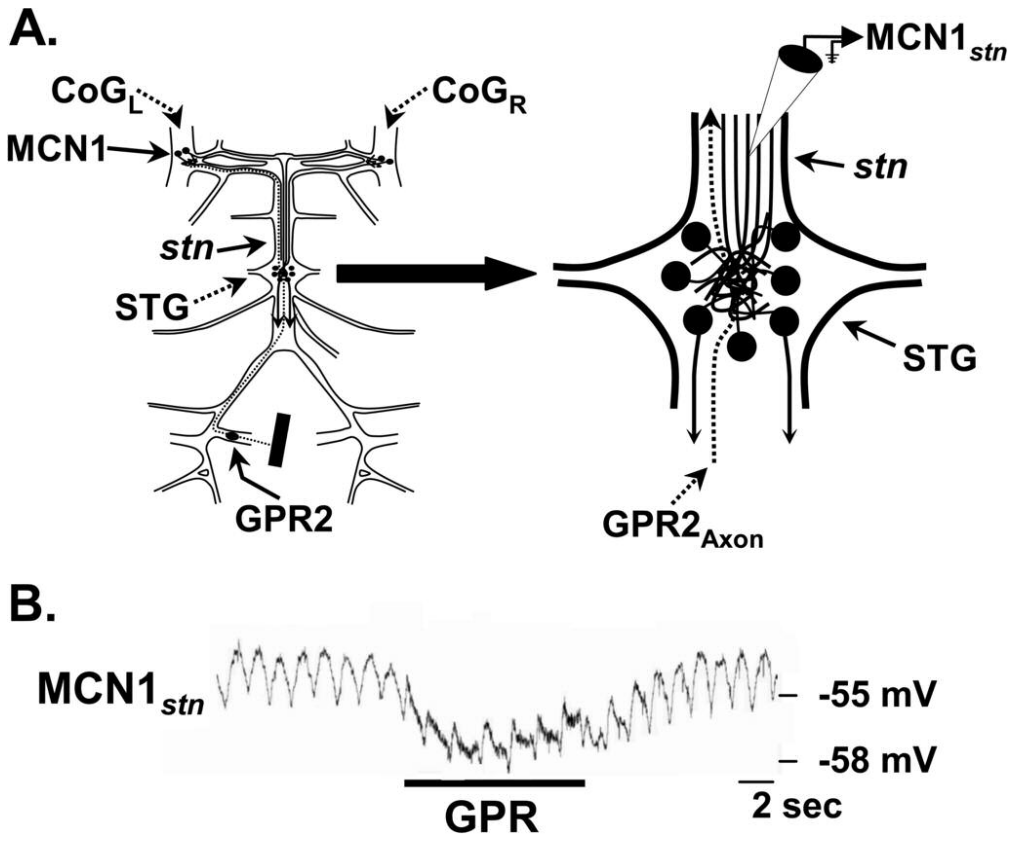

Figure 8. GPR stimulation hyperpolarizes the STG terminals of MCN1. A, Schematic of the isolated STNS (left), with an expanded view of the STG (right) to indicate the location of the intra-axonal recording site for MCN1stn. B, Intracellular recording of MCN1stn revealed a hyperpolarizing response to GPR stimulation (5 Hz). Note the subthreshold pyloric-timed oscillations in MCN1stn. The thickened MCN1stn trace during GPR stimulation represents the stimulus artifact.
86x71mm (300 x 300 DPI)

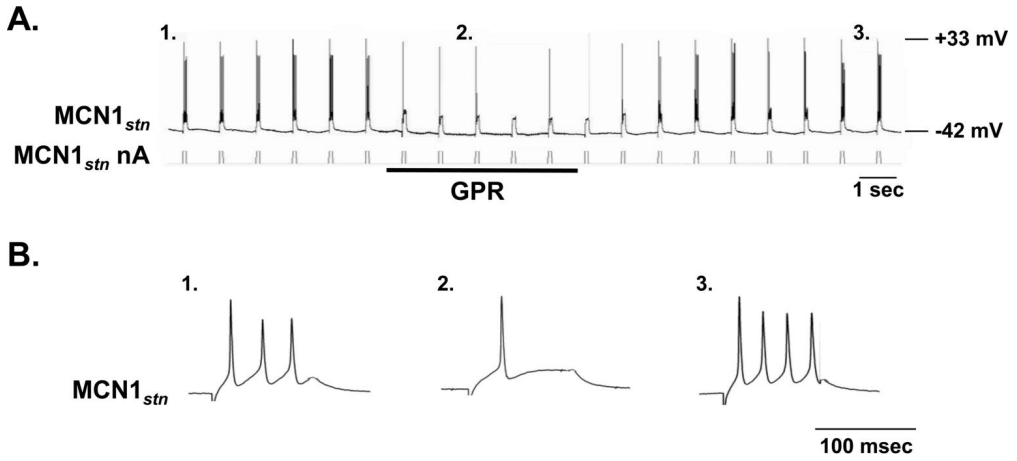

Figure 9. GPR stimulation inhibits MCN1 action potential initiation within the STG neuropil. A, Injecting depolarizing current into MCN1stn initiates action potentials within the STG neuropil (Coleman and Nusbaum, 1994). Constant duration (100 msec) and amplitude (+2nA) depolarizing pulses injected into MCN1stn produced a regular number (3-4) of action potentials/pulse. This number was reversibly reduced during GPR stimulation (5 Hz). Note the delay of several seconds after GPR stimulation before the number of MCN1 action potentials/pulse returns to control levels. B, Expanded traces from panel A of single pulses (1) before, (2) during and (3) after GPR stimulation.
129x58mm (300 x 300 DPI)

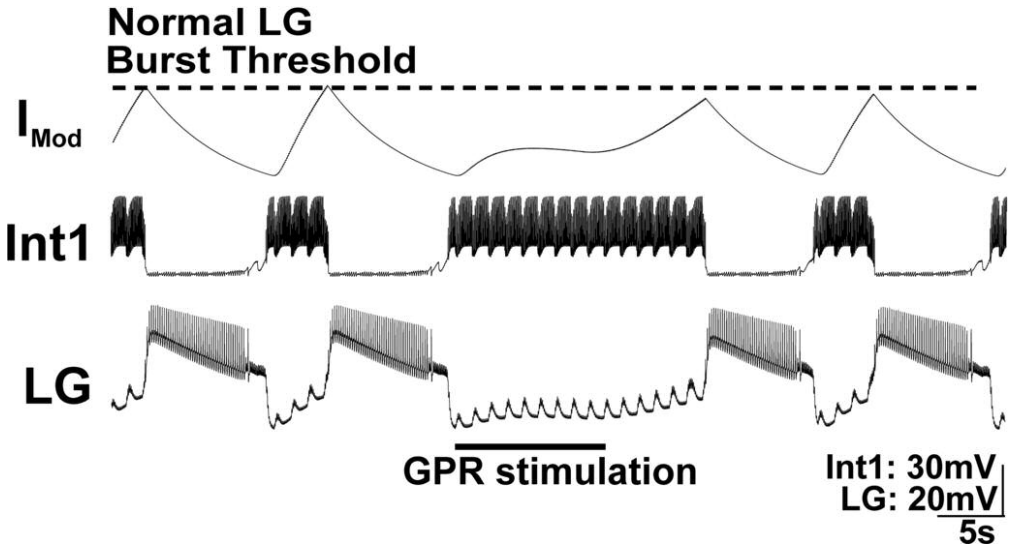

Figure 10. The GPR action on the MCN1-elicited gastric mill rhythm is best mimicked by GPR inhibition of MCN1STG in a computational model of the MCN1-elicited gastric mill rhythm. In this version of the model, GPR stimulation presynaptically inhibited MCN1STG, thereby reducing MCN1 actions onto the LG neuron. As a result, the amplitude of the modulatory current (IMod) induced in LG by MCN1 is reduced during GPR stimulation. This effect persists after GPR stimulation due to the slow time constant of the GPR action. The GPR inhibition of MCN1STG slowed the LG escape from Int1 inhibition, prolonging the retractor phase. Note that, in contrast, the protractor phase duration was not altered. Most hyperpolarized Vm: Int1, -65 mV; LG, -55 mV.
87x47mm (300 x 300 DPI)

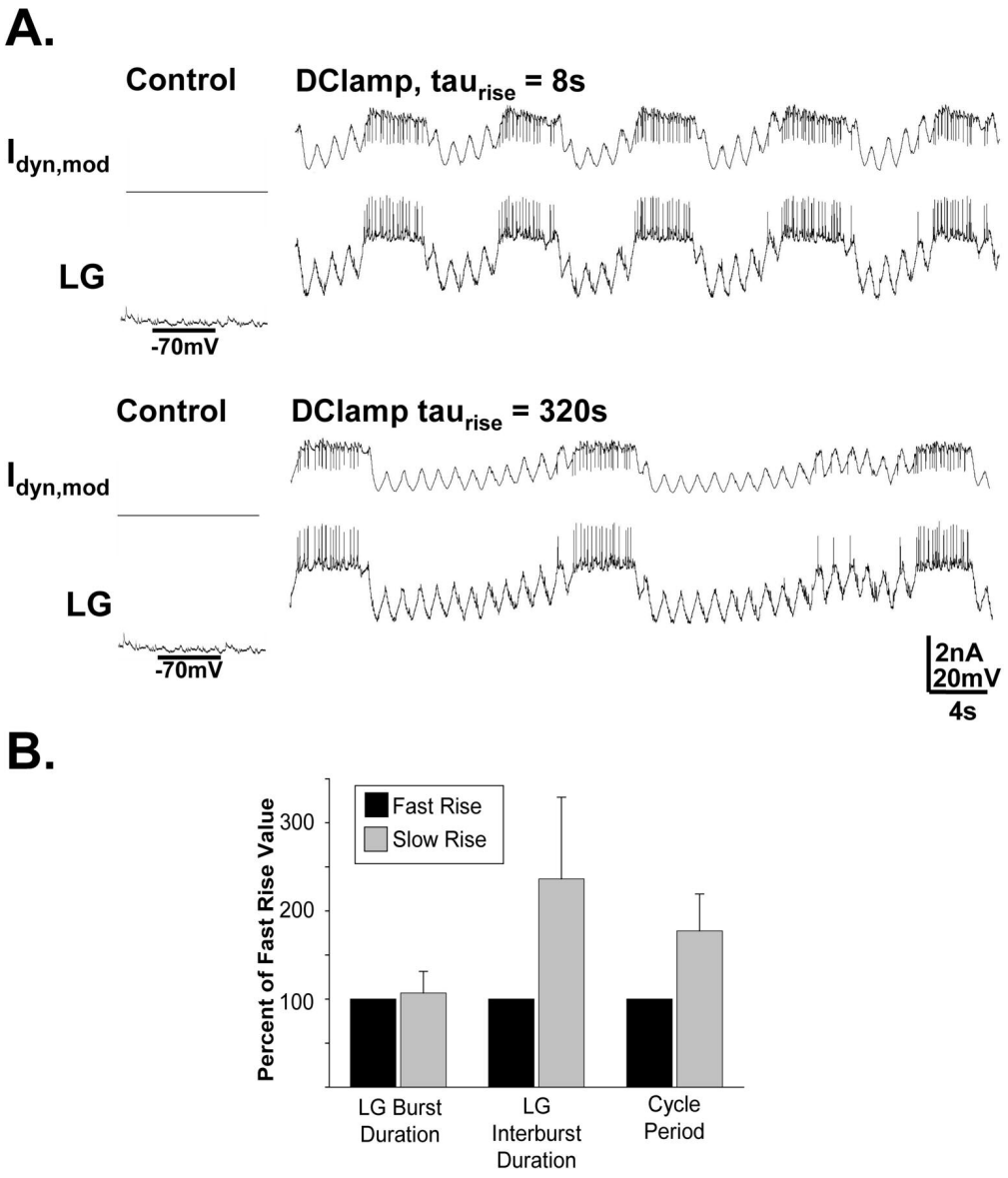

Figure 11. The rate of rise of MCN1-like modulation of the LG neuron selectively regulates the retractor phase duration. A, In this experiment, in place of MCN1 stimulation, the biological LG neuron was injected with a dynamic clamp version of the modulatory current that likely represents the current provided by MCN1 (Swensen and Marder, 2000; see Methods). The only parameter that differed during the dynamic clamp current injection in the two traces shown was the rate of rise of the current amplitude during each LG interburst. Note that the slower rate of rise (bottom trace) caused a slower rhythm, which resulted largely from a selectively prolonged LG interburst (retractor-like phase). Both LG traces are from the same preparation. B, Injecting the dynamic clamp version of the modulatory current into LG with a relatively long time constant for its rise in amplitude consistently elicited gastric mill-like activity in LG that was slower, due to a

selective increase in LG interburst duration, than that resulting from injection of the same current with a briefer time constant ($p<0.005$, $n=5$).
129x150mm (300 x 300 DPI)

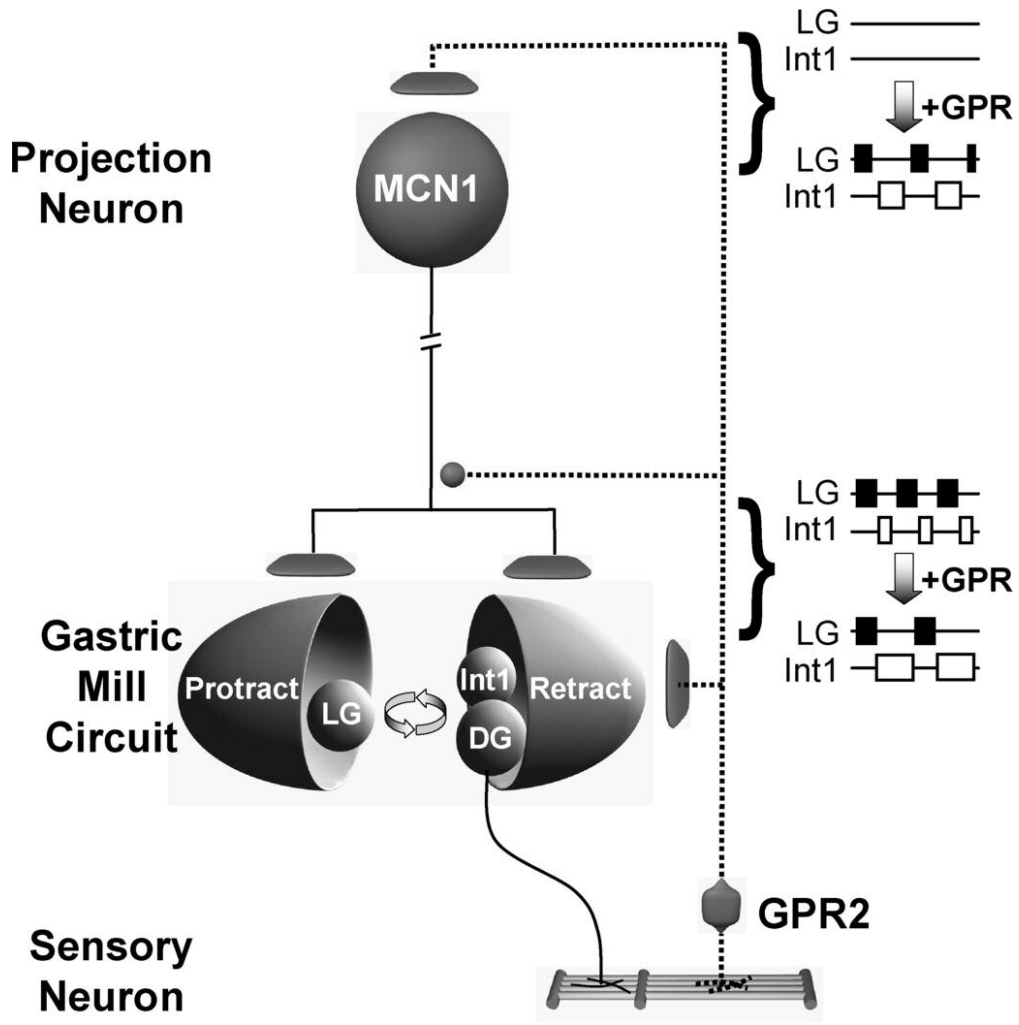

Figure 12. Working model of the GPR actions on the gastric mill system. Gastric mill-like rhythmic GPR stimulation can elicit the gastric mill rhythm (Blitz et al., 2004) by exciting the projection neuron MCN1 (and CPN2) in the commissural ganglia. During the gastric mill rhythm elicited by MCN1 (either directly or via activation of the VCN mechanosensory neurons), stimulating GPR in a behaviorally-appropriate manner (during each retractor DG neuron burst) slows the gastric mill rhythm by selectively prolonging the retractor phase. This latter GPR action results from GPR inhibition of the axon terminals of MCN1 in the stomatogastric ganglion, in concert with its excitation of the retractor neurons Int1 and DG. Synapse symbols: t-bars, excitation; filled circles, inhibition.
87x88mm (300 x 300 DPI)